AD_____

Award Number: W81XWH-10-1-0546

TITLE: Alterations of the Bone Marrow Microenvironment Contribute to Prostate Cancer Skeletal Metastasis

PRINCIPAL INVESTIGATOR: Dr. Serk In Park

CONTRACTING ORGANIZATION: The University of Michigan
Ann Arbor, MI 48109

REPORT DATE: May 2012

TYPE OF REPORT: Annual Summary

PREPARED FOR: U.S. Army Medical Research and Materiel Command
Fort Detrick, Maryland 21702-5012

REPORT DOCUMENTATION PAGE

Form Approved
OMB No. 0704-0188

1. REPORT DATE *(DD-MM-YYYY)*	2. REPORT TYPE	3. DATES COVERED *(From - To)*
01-05-2012	Annual Summary	15 APR 2011 - 14 APR 2012

4. TITLE AND SUBTITLE
Alterations of the Bone Marrow Microenvironment Contribute to Prostate Cancer Skeletal Metastasis

5a. CONTRACT NUMBER

5b. GRANT NUMBER
W81XWH-10-1-0546

5c. PROGRAM ELEMENT NUMBER

6. AUTHOR(S)
Dr. Serk In Park

E-Mail: serkinpark@hotmail.com

5d. PROJECT NUMBER

5e. TASK NUMBER

5f. WORK UNIT NUMBER

7. PERFORMING ORGANIZATION NAME(S) AND ADDRESS(ES)
The University of Michigan
Ann Arbor, MI 48109

8. PERFORMING ORGANIZATION REPORT NUMBER

9. SPONSORING / MONITORING AGENCY NAME(S) AND ADDRESS(ES)
U.S. Army Medical Research and Materiel Command
Fort Detrick, Maryland 21702-5012

10. SPONSOR/MONITOR'S ACRONYM(S)

11. SPONSOR/MONITOR'S REPORT NUMBER(S)

12. DISTRIBUTION / AVAILABILITY STATEMENT
Approved for Public Release; Distribution Unlimited

13. SUPPLEMENTARY NOTES

14. ABSTRACT

The purpose of this postdoctoral training grant was to provide the PI with opportunity to explore the metastatic bone microenvironment under the supervision of the mentor, Dr. Laurie McCauley, at the university of Michigan. The research plan of this proposal was to test a hypothesis that alterations of bone marrow microenvironment contribute to metastatic prostate cancer growth in bone. The specific aims were designed to investigate the contribution of hematopoietic cellular compartment in the bone marrow to the development of prostate cancer skeletal metastasis. This study demonstrated that alterations induced by cyclophosphamide, one of the most widely used chemotherapeutic drugs, enhanced bone metastasis in a prostate cancer animal model. Furthermore, this study showed that the pro-metastatic effects of cyclophosphamide were significantly reversed by suppression of CCL2, which suggests the causal role of bone marrow myeloid lineage cell expansion in promoting metastasis in the mouse model used in this study.

15. SUBJECT TERMS
Prostate cancer, metastasis, bone, bone marrow, microenvironment

16. SECURITY CLASSIFICATION OF:			17. LIMITATION OF ABSTRACT	18. NUMBER OF PAGES	19a. NAME OF RESPONSIBLE PERSON
a. REPORT	b. ABSTRACT	c. THIS PAGE			USAMRMC
U	U	U	UU	48	19b. TELEPHONE NUMBER *(include area code)*

Table of Contents

Page

Introduction……..…..….. **4**

Body…….. **4**

Key Research Accomplishments…….…….. **9**

Reportable Outcomes…… **10**

Conclusion…… **13**

References……. **14**

Appendices…… **15**

1. Introduction

The research plan of this proposal was to test a hypothesis that alterations of bone marrow microenvironment contribute to metastatic prostate cancer growth in bone. The specific aims were designed to investigate the contribution of hematopoietic cellular compartment in the bone marrow to the development of prostate cancer skeletal metastasis. The postdoctoral training plan was to provide the PI with opportunities to conduct scientific research on prostate cancer bone metastasis under the supervision of the mentor, Dr. Laurie K. McCauley in collaboration with other leading prostate cancer scientists in the University of Michigan.

2. Body

1. Training Accomplishments

This training grant has clearly contributed to the successful career development of the PI as an independent scientist dedicated to *prostate cancer research*. Based on the training supported by this award, the PI completed his postdoctoral training in prostate cancer skeletal metastasis with a recent employment as a tenure-track assistant professor in the Department of Medicine, Vanderbilt University School of Medicine. The PI will start an independent laboratory to extend his current research on the metastatic bone microenvironment of prostate cancer patients. In addition, the PI obtained a next-level independent research grant from the DOD-PCRP (FY2011 Exploration-Hypothesis Development Award). These outcomes strongly support the productive accomplishments of this training grant.

2. Research Accomplishments

The research accomplishments of this award over the course of 2-year support are described point-by-point according to the original Statement of Work (SOW). Because majority of the research outcomes are included in a recent publication in *Cancer Research* first-authored by the PI, detailed description of specific aspects of the research accomplishments is substituted with the published article.

Task 1: Quantitative analysis of the disrupted bone marrow sinusoidal vasculature (Specific Aim 2)
Timeline: months 1-2
Methods: Preliminary micro CT results will be quantitatively analyzed with computer software.
Outcomes: micro-vascular diameter, vascular distance, vascular density and volume
Results: Completed. Details of the results are described in the Figure 2 of the manuscript published in *Cancer Research* (Appendix No. 3).

Task 2: To determine the optimal dose of cyclophosphamide to specifically suppress the bone marrow cell population *in vivo* (Specific Aim 1)

Timeline: months 3-6

Methods: Mice will be pre-treated with varying doses of cyclophosphamide (25, 50, 100, 200, 200, 300 and 400 mg/kg), 7 days prior to analysis. At the time of analysis, the bone marrow cells will be flushed and the suppression of hematopoietic stem/progenitor cell will be determined by flow cytometry (Lineage$^-$Sca-1$^+$c-Kit$^+$ population) along with complete blood counting (WBC differential). In addition, bone marrow blood vasculature will be imaged to determine the integrity of the sinusoidal vascularity, and bone marrow vascular permeability will be measured.

Outcomes: Flow cytometric results of hematopoietic stem/progenitor cell population. Complete Blood Count. CT images of the bone marrow sinusoidal structure. Optical density of Evans Blue dye in the bone marrow extra-vascular space for vascular permeability.

Results: Completed.

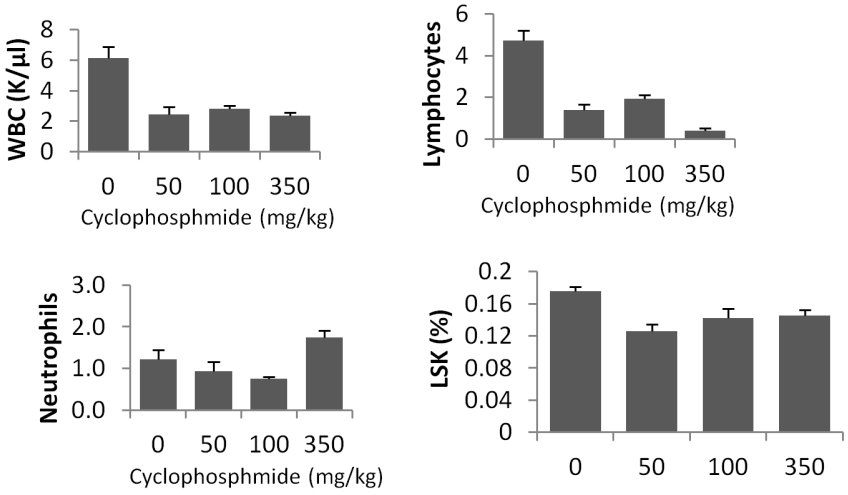

Male C57BL6 mice were treated with increasing doses of cyclophosphamide, followed by CBC and flow cytometric analyses of Lin$^-$Sca-1$^+$cKit$^+$ (LSK) cell populations after 7 days. All three doses (50, 100 and 350 mg/kg) of cyclophosphamide suppressed WBC, lymphocytes and LSK cells. However, only 350mg/kg significantly increased neutrophil counts. The subsequent experiments confirmed the causal role of the spike of neutrophils in cyclophosphamide-induced skeletal metastasis.

Micro-CT scanning and vascular permeability assay (using Evans blue dye) were not performed, based on the experimental results of *Tasks 4*. Briefly, the experiments in *Task 4* tested whether the vascular disruption contributes to the increased metastasis and/or tumor growth in bone. Contrary to the expectation, disruption of the vascular integrity in the bone marrow was not the primary factor in

cyclophosphamide-induced skeletal metastasis (Figure 3, Appendix No. 3). On the other hand, 350mg/kg cyclophosphamide significantly increased neutrophil counts after 7 days (see the above data figure), and our subsequent studies demonstrated that alterations in the neutrophils and the progenitor cells (myeloid-lineage cells) in the bone marrow contribute to the chemotherapy-induced skeletal metastasis. Accordingly, the research direction was adjusted to determine the role of myeloid cells in prostate cancer skeletal metastasis. Detailed description and discussion about the data are included in the *Cancer Research* publication (Appendix No. 3)

Task 3: To determine the effects of bone marrow suppression induced by cyclophosphamide on prostate cancer skeletal metastasis *in vivo* using an intra-cardiac PCa model (Specific Aim 1)
Timeline: months 7-10
Methods: male athymic mice will be pre-treated with cyclophosphamide (dose determined in ***Task 2***) 7 days before the experiment. Mice will be anesthetized with the Ketamine/Xylazine mixture. Mice will be placed in a supine position, and the thorax will be cleansed with 70% ethyl alcohol. Human prostate cancer cells detached from the sub-confluent culture will be suspended in Hank's balanced salt solution (200,000 cells in 100µl). Cell suspension will be injected into the left heart ventricle over 1 minute. Mice will be monitored for the vital signs until complete recovery from the anesthesia. Metastatic tumor incidence and growth will be measured by weekly *in vivo* bioluminescence imaging for six weeks. Tumors and serum will be harvested at the end of the experiment.
Outcomes: bioluminescence (tumor growth and incidence of metastasis), bone and tumor histomorphometry, serum biochemistry
Results: Completed. Details of the results are described in the Figure 1 of the manuscript published in *Cancer Research* (Appendix No. 3).

Task 4: To determine direct contribution of bone marrow cells to tumor growth using an intra-tibial prostate cancer injection model (Specific Aim 1)
Timeline: months 11-14
Methods: male athymic mice will be pre-treated with cyclophosphamide (dose determined in ***Task 2***) 7 days before the intra-tibial tumor cell inoculation. Mice will be anesthetized with the Ketamine/Xylazine mixture. Mice will be placed in a supine position, and the right hind limb will be cleansed with 70% ethyl alcohol. A hole will be made in the proximal tibia parallel to the long axis of the tibia, by drilling motion of 27½G needle attached to 1ml syringe. Human prostate cancer cell

suspension (100,000 cells in 20μl Hank's balanced salt solution) will be injected through the hole, and cotton will be applied to the injection site for 30 seconds. Mice will be monitored for vital signs until complete recovery from the anesthesia. Metastatic tumor incidence and growth will be measured by weekly *in vivo* bioluminescence imaging for six weeks. Tumors and blood serum will be harvested at the end of the experiment.

Outcomes: bioluminescence, bone and tumor histomorphometry, serum biochemistry

Results: Completed. Details of the results are described in the Figure 3 of the manuscript published in *Cancer Research* (Appendix No. 3).

Task 5: To determine vascular permeability induced by bone marrow disrupted agent(s) using Evans Blue *in vivo* permeability assay (Specific Aim 2)

Timeline: months 15-17

Methods: mice will be pre-treated with cyclophosphamide (dose determined in ***Task 2***) 7 days before the experiment. Mice will then be anesthetized with the Ketamine/Xylazine mixture. Evans Blue dye (30mg/ml in PBS) will be injected intra-venously (through tail vein, 45mg/kg). After 5 minutes, mice will be perfused with Linger's lactate solution supplemented with heparin for 5 minutes and femurs will be dissected. Bones will then be completely dried by vacuum dryer and dry weight will be measured. Extravasated Evans Blue dye in the bone will be eluted with 400μl formamide (at 70°C overnight). Optical absorbance at 620nm will be measured.

Outcomes: optical density

Results: Incomplete, and an alternative approach was employed. The experimental results of ***Task 4*** showed that the vascular disruption minimally affects the cyclophosphamide-induced bone metastasis. Accordingly, we decided not to perform this ***Task 5***. Alternatively, we determined the effects of cyclophosphamide on the bone marrow endothelial cell apoptosis. Briefly, we flushed the bone marrow of the saline- or cyclophosphamide-treated mice via TriZol reagent, followed by quantitative PCR for a CD31 endothelial cell marker. Cyclophosphamide-treated bone marrow had significantly reduced *Cd31* gene expression. In addition, we cultured the human bone marrow endothelial cells, and treated the cells with 4-hydroperoxycyclophosphamide (4-HC, a metabolite of cyclophosphamide with *in vitro* biological activity), followed by flow cytometric assay of apoptotic cells. 4-HC induced apoptosis of the bone marrow endothelial cells, suggesting the cyclophosphamide-induced vascular disruption is mediated by apoptosis of the bone marrow endothelium. The data are presented and detailed in the Figure 2 E and F of the manuscript published in *Cancer Research* (Appendix No. 3).

Task 6: To determine vascular permeability induced by bone marrow disrupted agent(s) using a human gene (Alu) probe-quantitative RT PCR (Specific Aim 2)
Timeline: months 18-20
Methods: mice will be pre-treated with cyclophosphamide (dose determined in ***Task 2***) 7 days before the intra-cardiac PCa tumor cell injection. Subsequently, five mice per group (pre-treatment vs. control) will be harvested weekly for six weeks. Bone marrow cells from the hind limbs will be flushed, and total RNA will be extracted using Trizol solution. cDNA will be synthesized by reverse transcription, and quantitative PCR with a human gene probe (Alu probe) will be performed.
Outcomes: Quantitative PCR measurement of a human gene (Alu probe)
Results: Incomplete. This task was contingent on the experimental results of the above ***Tasks 4*** and ***5*** that produced negative results. Accordingly, ***Task 6*** was determined not to pursue, and the alternative approaches (detailed in the Results of Task 5) were performed and presented.

Task 7: To determine angiogenic gene expression changes in the bone marrow and serum induced by bone marrow disruptive agent(s) by quantitative RT-PCR (Specific Aim 2)
Timeline: months 21-22
Methods: mice will be pre-treated with cyclophosphamide (dose determined in ***Task 2***, *n*=10 each group) 7 days before analysis. Animals will be sacrificed and serum and bone marrow flush will be harvested. Complete blood counting (with white blood cell differential) will be performed. Serum VEGF-A will be measured by ELISA. Total RNA will be extracted from the bone marrow flush cells, and quantitative RT-PCR will be performed to measure expression of angiogenic genes (VEGF-A, IL-6 and MCP-1).
Outcomes: Blood counts, ELISA and quantitative PCR measurement
Results: Completed. Details of the results are described in the Figure 4 of the manuscript published in *Cancer Research* (Appendix No. 3).

Task 8: Data analysis, review, repetition as needed. Manuscript preparation.
Timeline: months 23-24
Methods: Repeat and/or reanalyze experiments from all tasks as needed. Prepare manuscript for publication.
Outcomes: As described in the various tasks. A manuscript.
Results: Completed. An original research manuscript covering the tasks in this proposal was recently accepted for publication in *Cancer Research*.

3. Key Research Accomplishments

- Cyclophosphamide enhanced experimental prostate cancer skeletal metastasis in vivo
- A single dose of cyclophosphamide significantly disrupted bone marrow vascular integrity
- Cyclophosphamide pre-treatment promoted orthotopic prostate tumor growth in bone
- Cyclophosphamide transiently expanded myeloid lineage cells
- Cyclophosphamide-induced skeletal metastases overlap temporally with bone marrow myeloid cell expansion
- Neutralizing host-derived murine CCL2, but not murine IL-6, inhibited cyclophosphamide-induced prostate cancer bone metastasis
- An alternative chemotherapeutic drug, docetaxel, did not promote skeletal metastases

4. Reportable Outcomes

The successful outcomes of this postdoctoral training grant are readily apparent through one review paper, two original research papers, two oral presentations in international conferences, and four awards to the PI. More importantly, during the later period of this grant support, Dr. Park was awarded with an independent research grant from the DOD PCRP (FY 2011 Exploration-Hypothesis Development Award). In addition, Dr. Park is recently appointed as a tenure-track assistant professor in the Department of Medicine, Vanderbilt University School of Medicine, indicating his successful career progression in the field of prostate cancer research.

One review paper

1. A review article published in *Cancer Microenvironment*: "Roles of Bone Marrow Cells in Skeletal Metastases: No Longer Bystanders" This review article was written by the PI (as the first author) in collaboration with the mentor (the corresponding author), with an acknowledgement of funding supports from this grant.

Two original research papers

2. An original research article published in *Endocrine-Related Cancer*: "Nuclear Localization of Parathyroid Hormone-related Peptide Confers Resistance to Anoikis in Prostate Cancer Cells" Works in this manuscript were partly supported by this postdoctoral fellowship grant, which was acknowledged in the text. The PI is the first author of this publication.
3. An original research article accepted for publication in *Cancer Research*: "Cyclophosphamide Creates a Receptive Microenvironment for Prostate Cancer Skeletal Metastasis", which was partly supported by this grant. The manuscript is currently in press, of which the PI is the first author.

Six presentations with four awards

4. Poster presentation
    1. The 9th International Meeting on Cancer-Induced Bone Disease
    2. October 27-29, 2009, Arlington, VA

3. Title: Chemotherapy-induced alterations of the bone marrow microenvironment contribute to prostate cancer skeletal metastasis
4. Authors: Serk In Park, Jinhui Liao, Xin Li, Jan Berry, Matthew Eber, and Laurie K. McCauley

5. Poster presentation
    1. 2010 American Association for Cancer Research Annual Meeting
    2. April 17-21, 2010, Washington DC
    3. Title: Novel insight into mechanisms of parathyroid hormone-related protein (PTHrP) action in prostate cancer growth and skeletal metastasis: altered anoikis and angiogenesis
    4. Authors: Serk In Park, Xin Li, Janice E. Berry, Amy J. Koh, Jingcheng Wang, Russell S. Taichman, and Laurie K. McCauley
6. Poster presentation
    1. 2011 IMPaCT Meeting
    2. March 9-12, 2011, Orlando, FL
    3. Title: Cyclophosphamide-induced expansion of CD11b+ myeloid cells contribute to prostate cancer skeletal metastasis
    4. Authors: Serk In Park, Jinhui Liao, Janice E. Berry, Xin Li, Fabiana N. Soki, Sudha Sud, Kenneth J. Pienta, and Laurie K. McCauley
7. Oral presentation
    1. 2011 Annual Meeting of the American Society of Bone and Mineral Research (ASBMR)
    2. September 16-19, 2011, San Diego, CA
    3. Title: Parathyroid Hormone-related Peptide (PTHrP) Up-regulates Myeloid-Derived Suppressor Cells (MDSC) in the Bone Marrow, Contributing to Prostate Cancer Growth and Angiogenesis
    4. Authors: Serk In Park, Willam D. Sadler, Amy J. Koh, Fabiana N. Soki and Laurie K. McCauley
8. Young Investigator Travel Award from the ASBMR
9. Poster presentation
    1. Endocrine Fellows Foundation Forum
    2. September 14-15, San Diego, CA
    3. Title: Parathyroid Hormone-related Peptide (PTHrP) Up-regulates Myeloid-Derived Suppressor Cells (MDSC) in the Bone Marrow, Contributing to Prostate Cancer Growth and Angiogenesis
    4. Authors: Serk In Park, Willam D. Sadler, Amy J. Koh, Fabiana N. Soki and Laurie K. McCauley

10. Travel award from the Endocrine Fellows Foundation
11. Oral presentation
    1. The 11th International Conference on Cancer-Induced Bone Disease
    2. November 30-December 3, Chicago, IL
    3. Title: Potentiation of Myeloid-Derived Suppressor Cells (MDSCs) within the Bone Marrow by Tumor-Derived Parathyroid Hormone-related Peptide (PTHrP)
    4. Authors: Serk In Park, Willam D. Sadler, Amy J. Koh, Fabiana N. Soki, and Laurie K. McCauley
12. Young Investigator Travel Award and a "Short Talk Presentation Award" from the International Conference on Cancer-Induced Bone Disease

One research funding

13. FY2011 Department of Defense Prostate Cancer Research Program, Exploration-Hypothesis Development Award

Employment

14. Employment as a tenure-track Assistant Professor in the Department of Medicine, Vanderbilt University School of Medicine, Nashville, TN. The PI has a joint appointment in the Department of Cancer Biology.

5. Conclusions

This study demonstrated for the first time that alterations induced by cyclophosphamide, one of the most widely used chemotherapeutic drugs, enhanced bone metastasis in a prostate cancer animal model. Furthermore, this study showed that the pro-metastatic effects of cyclophosphamide were significantly reversed by suppression of CCL2, which suggests the causal role of bone marrow myeloid lineage cell expansion in promoting metastasis in the mouse model used in this study. We demonstrated that a single dose of cyclophosphamide administration increased myelogenic cytokines, and correspondingly expanded the myeloid cell population in the bone marrow, as well as the numbers of monocytes and neutrophils transiently in the peripheral blood.

6. References

1. Carmel RJ, Brown JM. The effect of cyclophosphamide and other drugs on the incidence of pulmonary metastases in mice. Cancer Res. 1977 Jan;37(1):145-51.

2. Man S, Zhang Y, Gao W, Yan L, Ma C. Cyclophosphamide promotes pulmonary metastasis on mouse lung adenocarcinoma. Clin Exp Metastasis. 2008;25(8):855-64.

3. Wu YJ, Muldoon LL, Dickey DT, Lewin SJ, Varallyay CG, Neuwelt EA. Cyclophosphamide enhances human tumor growth in nude rat xenografted tumor models. Neoplasia. 2009 Feb;11(2):187-95.

4. Yamauchi K, Yang M, Hayashi K, Jiang P, Yamamoto N, Tsuchiya H, et al. Induction of cancer metastasis by cyclophosphamide pretreatment of host mice: an opposite effect of chemotherapy. Cancer Res. 2008 Jan 15;68(2):516-20.

5. Bagley CM, Jr., Bostick FW, DeVita VT, Jr. Clinical pharmacology of cyclophosphamide. Cancer Res. 1973 Feb;33(2):226-33.

6. Kline I, Gang M, Tyrer DD, Mantel N, Venditti JM, Goldin A. Duration of drug levels in mice as indicated by residual antileukemic efficacy. Chemotherapy. 1968;13(1):28-41.

7. Shirota T, Tavassoli M. Cyclophosphamide-induced alterations of bone marrow endothelium: implications in homing of marrow cells after transplantation. Exp Hematol. 1991 Jun;19(5):369-73.

8. Butcher JT, Sedmera D, Guldberg RE, Markwald RR. Quantitative volumetric analysis of cardiac morphogenesis assessed through micro-computed tomography. Dev Dyn. 2007 Mar;236(3):802-9.

9. Guldberg RE, Duvall CL, Peister A, Oest ME, Lin AS, Palmer AW, et al. 3D imaging of tissue integration with porous biomaterials. Biomaterials. 2008 Oct;29(28):3757-61.

10. Kopp HG, Avecilla ST, Hooper AT, Shmelkov SV, Ramos CA, Zhang F, et al. Tie2 activation contributes to hemangiogenic regeneration after myelosuppression. Blood. 2005 Jul 15;106(2):505-13.

11. Ferrara N, Gerber HP, LeCouter J. The biology of VEGF and its receptors. Nat Med. 2003 Jun;9(6):669-76.

12. Kim S, Takahashi H, Lin WW, Descargues P, Grivennikov S, Kim Y, et al. Carcinoma-produced factors activate myeloid cells through TLR2 to stimulate metastasis. Nature. 2009 Jan 1;457(7225):102-6.

13. Roca H, Varsos ZS, Sud S, Craig MJ, Ying C, Pienta KJ. CCL2 and interleukin-6 promote survival of human CD11b+ peripheral blood mononuclear cells and induce M2-type macrophage polarization. J Biol Chem. 2009 Dec 4;284(49):34342-54.

7. Appendices

1. A review article published in *Cancer Microenvironment*: “Roles of Bone Marrow Cells in Skeletal Metastases: No Longer Bystanders”
2. An original article published in *Endocrine-Related Cancer*: “Nuclear Localization of Parathyroid Hormone-related Peptide Confers Resistance to Anoikis in Prostate Cancer Cells”
3. An original article accepted for publication in *Cancer Research*: “Cyclophosphamide Creates a Receptive Microenvironment for Prostate Cancer Skeletal Metastasis.” Because the manuscript is currently in press, a copy of author proof was provided, and this is not to be released to the public.

Cancer Microenvironment
DOI 10.1007/s12307-011-0081-8

ORIGINAL PAPER

Roles of Bone Marrow Cells in Skeletal Metastases: No Longer Bystanders

Serk In Park · Fabiana N. Soki · Laurie K. McCauley

Received: 20 May 2011 / Accepted: 20 July 2011

Abstract Bone serves one of the most congenial metastatic microenvironments for multiple types of solid tumors, but its role in this process remains under-explored. Among many cell populations constituting the bone and bone marrow microenvironment, osteoblasts (originated from mesenchymal stem cells) and osteoclasts (originated from hematopoietic stem cells) have been the main research focus for pro-tumorigenic roles. Recently, increasing evidence further elucidates that hematopoietic lineage cells as well as stromal cells in the bone marrow mediate distinct but critical functions in tumor growth, metastasis, angiogenesis and apoptosis in the bone microenvironment. This review article summarizes the key evidence describing differential roles of bone marrow cells, including hematopoietic stem cells (HSCs), megakaryocytes, macrophages and myeloid-derived suppressor cells in the development of metastatic bone lesions. HSCs promote tumor growth by switching on angiogenesis, but at the same time compete with metastatic tumor cells for occupancy of osteoblastic niche. Megakaryocytes negatively regulate the extravasating tumor cells by inducing apoptosis and suppressing proliferation. Macrophages and myeloid cells have pro-tumorigenic roles in general, suggesting a similar effect in the bone marrow. Hematopoietic and stromal cell populations in the bone marrow, previously considered as simple by-standers in the context of tumor metastasis, have distinct and active roles in promoting or suppressing tumor growth and metastasis in bone. Further investigation on the extended roles of bone marrow cells will help formulate better approaches to treatment through improved understanding of the metastatic bone microenvironment.

Keywords Bone marrow · Metastasis · Hematopoietic stem cells · Megakaryocytes · Macrophages · Myeloid-derived suppressor cells

S. I. Park · F. N. Soki · L. K. McCauley (✉)
Department of Periodontics and Oral Medicine,
The University of Michigan School of Dentistry,
1011 N. University Avenue,
Ann Arbor, MI 48109, USA
e-mail: mccauley@umich.edu

L. K. McCauley
Department of Pathology,
The University of Michigan Medical School,
Ann Arbor, MI, USA

Introduction

The majority of cancer patients ultimately develop metastatic lesions, contributing to excessive morbidity and mortality, even though metastasis is a very selective and extremely inefficient process, with less than 0.1% of the intravasated tumor cells surviving cascades of events to form metastatic lesions in distant sites [1, 2]. More importantly, tumor metastasis is determined not by locoregional anatomy of draining vasculature (i.e. hemodynamic factors), but by highly specific interactions between disseminating tumor cells ("seed") and the microenvironment of the target organ ("soil") [3]. This seminal concept of "seed and soil" was originally proposed by Stephen Paget in the 19th century [4], but soon challenged by Ewing and many others proposing that mechanical forces and hemodynamic factors determine the metastatic patterns [1, 5, 6]. Later, the "seed and soil" hypothesis was revisited by central evidence that the primary tumor is comprised of biologically heterogeneous cell populations (i.e. subpopulations of different metastatic potentials), and also that metastases selectively develop in congenial microenvironments regardless of hemodynamic trafficking [7, 8]. In addition, Tarin et al. provided clinical

Published online: 02 August 2011

evidence that the specific organ microenvironment is a critical determinant in metastasis, independent of vascular anatomy, rate of blood flow and the number of tumor cells delivered to the organ [9, 10]. Indeed, the current cancer statistics clearly show that the primary tumors of individual organs have strong preference for their metastatic sites [11, 12]. For example, colon and pancreatic tumors preferentially metastasize to liver; and renal cell carcinoma and bladder cancer frequently spread to lungs. Therefore, tumor metastasis occurs in a predictable manner, tightly regulated by the microenvironment of the recipient organ.

Interestingly, bone is the predominant metastatic soil for a number of human cancers, including prostate, breast and lung cancers as well as multiple myeloma [11, 13, 14]. Skeletal metastasis is the major cause of mortality and morbidity of afflicted patients. For example, approximately 90% of advanced stage prostate cancer patients develop bone lesions, resulting in morbidities such as severe bone pain, immobility, hematopoietic complications and spinal cord compression [12, 15]. Current treatment modalities for bone metastatic lesions are not curative, and the average time from the surgery (for bone lesions, such as pathologic fracture) to death is only 1.5±1.9 years for prostate cancer patients. To overcome this urgent clinical problem, better understanding of the metastatic bone microenvironment is critically important. Bone is an intriguing microenvironment for tumor biology, and still remains largely unexplored [16]. This uniquely complex milieu is due not only to the calcified matrix but also to multiple types of constituting cells, including bone cells (osteocytes, osteoclasts and osteoblasts), hematopoietic cells, immune cells, stromal cells and endothelial cells [17]. Considerable research efforts have been devoted to characterizing this complex microenvironment and also to elucidating differential roles of individual cell types in their contribution to tumor growth and metastasis in bone [13]. Notably, Mundy and colleagues proposed a 'vicious cycle' theory which involves bi-directional interactions between disseminated tumor cells and osteoclasts (as well as osteoblasts) leading to osteolysis and, in turn, tumor growth [13, 18, 19]. For example, parathyroid hormone-related peptide (PTHrP) derived from breast cancer cells promotes osteolytic bone lesions (mediated by activation of osteoclasts), leading to release of transforming growth factor-beta (TGF-β) from the bone matrix to further aggravate tumor growth in the bone [18, 19]. Later, prostate cancer cells were shown to express PTHrP in order to upregulate expression of tumorigenic factors (such as C-C chemokine ligand 2 [CCL2]) in osteoblasts, resulting in destructive cascades in the bone as well as osteoblastic lesions [20–22]. However, the majority of experimental results are from murine models, and the vicious cycle in human breast/prostate cancer skeletal metastases is lacking yet difficult to discern.

Collectively, the current data demonstrate a positive feedback loop of tumor cell interaction with the hard tissue compartment of the bone microenvironment (i.e. osteoclasts, osteoblasts and calcified bone matrix). Additionally, however, current evidence suggests that different hematopoietic lineage cell populations in the bone marrow, previously considered as simple bystanders in the metastatic process, provide distinctive contributions for promoting or suppressing tumor growth and/or metastasis [23, 24]. This review paper will examine the current literature regarding cells in the bone microenvironment, with particular focus on hematopoietic lineage cells in the bone marrow, and their roles in skeletal metastasis.

Cellular Components of the Congenial Soil: Anatomy and Histology of Bone Marrow

The bone marrow is one of the largest organs in the human body, and comprises approximately 5% of body weight in humans and 3% in adult rats [25, 26]. Bone marrow is the primary hematopoietic organ and a primary lymphoid tissue, responsible for the production of the cellular components of blood [27]. It consists of hematopoietic tissue, endosteum, connective tissue and endothelium. The endosteal lining in the marrow cavity contains a single layer of cells, including osteoblasts and osteoclasts, supported by a thin layer of reticular connective tissue. Other connective tissues in the bone marrow include bony trabeculae, adipocytes, fibroblasts and nerves. Of particular note, the bone marrow is extremely well vascularized tissue, served by multiple arteries entering the marrow via nutrient canals of diverse size. Arteries branch and taper down to thin-walled arterioles and capillaries anastomosing with a plexus of venous sinuses. Venus sinuses then merge to form collecting veins and further the central venous sinus draining back via nutrient canals into the systemic circulation. Sinusoidal vessels are thin-walled, consisting of a layer of flat endothelial cells with little to no basement membrane. Bone marrow sinusoids function as an entering point for hematopoietic cells into the systemic circulation. Similarly, metastatic cancer cells are considered to extravasate via sinusoidal barrier. The bone marrow does not have a lymphatic drainage system [27–29].

The hematopoietic compartment of the bone marrow is comprised of stem cells, hematopoietic lineage cells, adventitial reticular cells, adipocytes and macrophages. Hematopoietic cells are not randomly dispersed, but are structured within the microenvironment [30]. More importantly, hematopoiesis occurs as a compartmentalized process, with erythropoiesis occurring in erythroblastic islands; granulopoiesis in less defined areas and megakaryopoiesis adjacent to the sinus endothelium. On demand, the hematopoietic cells transverse the sinusoidal barrier to enter the

systemic circulation, whereas platelets are released directly from the cytoplasm of megakaryocytes into the bloodstream.

During embryonic development, hematopoiesis occurs in the liver, and shortly after birth hematopoietic stem cells (HSCs) migrate and repopulate the bone marrow. This unique feature of bone marrow biology, bone marrow homing, has been extensively exploited clinically to improve the engrafting efficiency of bone marrow transplantation, carried out by simple intravenous injection of marrow cells [31]. Molecular mechanisms of bone marrow homing have been demonstrated primarily by exploring factors inhibiting homing in various mouse models. For example, mice deficient in E- and P-selectins were found to have impaired homing, suggesting that tethering and rolling of bone marrow cells on the sinusoidal endothelium is critical for correct engraftment [32, 33]. More importantly, Peled et al. provide pivotal evidence that stromal-derived factor-1 (SDF-1, also known as CXCL12) expressed by the bone marrow stroma and endothelium interacts with its cognate ligand, CXCR-4 expressed on HSCs, is critical to human HSC engraftment and repopulation in a immune-deficient mouse model [34]. In sum, the bone marrow is structured hierarchically, containing various populations of hematopoietic cells supported by stromal cells, all of which potentially have unique function in skeletal tumor growth and/or metastasis.

Hematopoietic Stem Cells Compete with Metastatic Tumor Cells

Tumor cells frequently usurp physiological mechanisms to promote growth, angiogenesis, invasion and metastasis. For example, most of the so-called tumorigenic molecules (such as vascular endothelial growth factor [VEGF], matrix metalloproteinases [MMPs] and epidermal growth factor [EGF] among myriad others) play critical roles in normal physiology and development. As stated above, liver is the primary hematopoietic organ until birth, and subsequently HSCs migrate into the bone marrow where the microenvironment supports engraftment, repopulation and self-renewal. This phenomenon of physiological HSC homing in the bone marrow led scientists to an interesting hypothesis that bone metastatic cancer cells may mimic the established pathway of HSC homing. Müller et al. for the first time provided pivotal evidence that chemokine receptors (CXCR4 and CCR7, highly expressed by breast cancer cells) and their cognate ligands (expressed in metastatic recipient tissues) play critical roles in organ-specific breast cancer metastasis [35], in the same way that chemokine-chemokine receptor axes mediate HSC homing in the bone marrow during normal development and bone marrow transplantation (BMT). Subsequently, Taichman et al. demonstrated that CXCL12/SDF-1 (expressed by osteoblasts and endothelial cells) and its receptor (CXCR4, expressed by prostate cancer cells) regulate bone-tropism of prostate cancer cells [36]. In addition to the CXCL12/CXCR4/CXCR7 axis [37], Annexin II, expressed by osteoblasts and endothelium regulates HSC adhesion, homing and engraftment [38]. Interestingly, human prostate cancer cells isolated from the metastatic lesions (PC-3, DU145 and LNCaP) were shown to express receptors for Annexin II, contributing to prostate cancer growth and homing in the bone marrow [39]. Given that data collectively demonstrated that bone metastatic tumor cells (breast and prostate) utilize the chemokine axes of HSC homing, it is reasonable to expect that HSCs may compete with metastatic cancer cells for occupancy in the bone marrow.

Recently, crucial evidence demonstrating that hematopoietic stem cells (HSC) negatively regulate bone metastasis by competing with metastatic cancer cells to preoccupy the HSC endosteal niche came from the works of Shiozawa et al. [40] The authors demonstrated that increasing the HSC niche size (i.e. expansion of osteoblasts by parathyroid hormone [PTH] treatment) promoted skeletal localization of prostate cancer cells in the systemic circulation, while decreasing the niche size (using a conditional osteoblast-ablation mouse model) reduced tumor cell number localized in the bone marrow. In addition, an experimental treatment to mobilize HSCs (AMD3100, similarly to a clinical regimen used in autologous stem cell transplantation) could mobilize the cancer cells in the niche back into the circulation. Therefore, the HSC endosteal niche serves as a direct target for metastatic prostate cancer cells, and HSCs may function as competitors for metastatic cancer cells with strong bone tropism.

Contrary to the data demonstrating HSCs function as a competitor for niche occupancy, other data shows that HSCs may directly promote tumor growth and/or metastasis. Okamoto et al. demonstrated that HSCs regulate the angiogenic switch and promote tumor growth in the bone [41]. Furthermore, expansion of bone marrow cellularity by treatment with parathyroid hormone (PTH) resulted in significantly increased prostate cancer cell localization and subsequent growth in bone [42]. HSCs are pluripotent cells that can differentiate into any hematopoietic lineage cell types of tumorigenic potential. Accordingly, the direct roles of HSCs in tumor growth, particularly in the context of the bone microenvironment, need further investigation.

Megakaryocytes Attack Extravasating Tumor Cells in the Bone Marrow

As previously mentioned, megakaryocytes reside in para-sinusoidal space with cytoplasmic invagination across the vascular barrier. As a result, platelets are released directly

into the sinusoidal venous blood [43]. Because the sinusoidal endothelium is the main entry-exit point between the circulation and bone marrow tissue, bone metastatic cancer cells are thought to utilize the same route to extravasate. Therefore, megakaryocytes are potentially the first cells that tumor cells encounter upon arrival in the bone marrow microenvironment. Interestingly, Li et al. provided the first direct data that megakaryocytes suppress tumor cell proliferation and increase apoptosis in an experimental prostate cancer bone metastasis model [44]. In addition, expansion of the megakaryocyte population (by administering recombinant thrombopoietin) resulted in significantly reduced localization of tumor cells and subsequent growth in the bone in vivo. Direct contact between prostate cancer cells and megakaryocytic cells in vitro resulted in increased apoptosis as well as decreased proliferation of prostate cancer cells. These results demonstrated novel and specific inhibitory effects of megakaryocytes, a specialized hematopoietic lineage cell residing in the bone marrow, on metastatic cancer growth in the bone.

In parallel to tumor inhibitory effects based on direct cell-to-cell contact, secretory factors from megakaryocytes have been recently demonstrated to suppress osteoclast formation and activation [45–47]. In addition, megakaryocytes promote osteoblast synthesis of type I collagen, osteoprotegerin and receptor activator of nuclear factor kappa-B ligand (RANKL), all of which positively affect bone formation [48]. Reciprocally, osteoblasts directly influence hematopoiesis [49, 50] as well as megakaryopoiesis [51]. Consequently, production and activity of megakaryocytes are tightly coupled with bone remodeling, which in turn affects tumor growth in the bone. Given that the vicious cycle theory integrates activities of osteoblasts and osteoclasts as critical components [13], and that resorption is essential for tumor growth in bone [20, 52], megakaryocytes also alter the bone microenvironment (i.e. suppressing osteoclasts and activating osteoblasts) to affect metastatic tumor growth indirectly. Taken together, the current data suggest that megakaryocytes negatively regulate tumor cells in the bone marrow directly by suppressing tumor cell proliferation and inducing apoptosis, and also indirectly by suppressing osteoclasts and osteoblasts. However, detailed molecular mechanisms and clinical data are required to further characterize the role of megakaryocytes in skeletal metastasis.

Contrary to anti-metastatic functions of megakaryocytes, the end-products, platelets, have been shown to have opposite roles. Firstly, platelet-derived growth factor (PDGF) is one of the first angiogenic factors discovered, and critical to vessel maturation [53]. In addition, aggregation of platelets surrounding tumor cells had been shown to protect tumor cell lysis by natural killer cells [54]. Most notably, Boucharaba et al. provided pivotal evidence supporting the role of platelets in breast cancer skeletal metastasis [55, 56]. Activation of platelets by tumor cells result in production of lysophosphatidic acid (LPA), which in turn promotes breast cancer growth and skeletal metastasis in mice [55]. However, there is currently no clear evidence supporting clinical benefits of anti-platelet agents (such as aspirin and heparin) in cancer patients [56].

Macrophages Promote Tumor Growth and Metastasis in Bone: More than a Scavenger

Increasing evidence now clearly supports that tumor-associated macrophages (TAMs) are important regulators of tumor progression in multiple types of cancers [57–61]. Clinical studies reveal that the density of TAMs in tumor tissue significantly correlates with poor prognosis in prostate, breast, ovarian and cervical cancers, and with controversial outcomes in stomach and lung cancers [62]. In comparison with classically activated macrophages (M1 macrophages) associated with inflammatory phagocytosis, TAMs are an alternatively activated and polarized population of macrophages (M2 macrophages) with tumorigenic potential [63]. The role of immune cells, particularly macrophages, in tumor progression is not a new idea. The first suggestion of their involvement dates back to 1863 [64]. Recent studies now provide the clinical correlations as well as potential molecular mechanisms of recruitment, activation and function of TAMs (M2 macrophages). In particular, most prominent molecules produced by tumors to affect TAMs include C-C chemokine ligand 2 (CCL2, also known as monocyte chemoattractant protein-1 [MCP-1]), macrophage colony stimulating factor (M-CSF, also known as CSF-1) and VEGF. For example, bone metastatic prostate cancer cells express CCL2 to recruit monocytes to tumor sites, which then differentiate into TAMs (M2 macrophages) and osteoclasts [58, 65–67]. In addition, CCL2 has been seen to increase prostate cancer growth and bone metastasis in an experimental metastasis model, which was accompanied by the recruitment of macrophages and osteoclasts [57, 68]. Lin et al. also demonstrated that macrophages switch on tumor angiogenesis, using the polyoma middle-T antigen mouse mammary tumor (PyMT) spontaneous breast cancer model [69]. Macrophages are highly specialized phagocytic cells, derived from monocytes. In tumor tissue, a wide variety of factors are secreted by tumor cells, including those that function as recruiting factors for monocyte-macrophages. The most prominent and widely investigated functions of TAMs (M2 macrophages) in tumor tissue are increased angiogenesis and tumor growth caused by growth factors and proteinases. Data of Harris et al. showed by immunohistochemical quantification that TAMs cluster in areas of increased angiogenesis in human breast cancer samples [70]. In addition, TAMs (M2 macrophages) produce many pro-angiogenic cytokines such as urokinase-type plasminogen activator (uPA)[71], tumor

necrosis factor-alpha (TNF-α)[72], IL-1, VEGF [73] and nitric oxide (NO)[74]. Moreover, TAMs express a wide variety of growth factors and proteinases such as MMP-7 and 9; fibroblast growth factor (FGF), hepatocyte growth factor (HGF), epidermal growth factor (EGF) and platelet-derived growth factor (PDGF), all of which have independent pro-tumorigenic functions [75–77].

Recently, interesting data from Pettit and colleagues demonstrated that a discrete population of macrophages, osteal tissue macrophages (termed 'OsteoMacs'). Later, the authors also showed that OsteoMacs are required for physiological bone remodeling as well as intramembranous bone healing, suggesting that osteal macrophages are critical components in bone physiology [78, 79]. However, there is currently no definitive data showing the tumorigenic function of resident macrophages in tumor growth and/or metastasis in bone. To sum up, clinical and experimental data supports the tumorigenic roles of macrophages in primary tumor tissue, but further investigation is required for the potential roles in the bone microenvironment.

Myeloid-Derived Suppressor Cells and Monocytes: An Elusive Population with Confronting Functions

As frequently portrayed as 'wounds that never heal', cancer is comprised of multiple types of immune/inflammatory cells [80]. Clinical data have now accumulated indicating that human tumor samples positively correlate with infiltration of bone marrow-derived immune cells (BMDCs) such as macrophages and neutrophils. In particular, recent evidence collectively shows that bone marrow-derived macrophages and monocytes (collectively termed 'myeloid lineage cells') play crucial roles in tumor angiogenesis [76, 81, 82]. However, those pro-angiogenic myeloid cells are yet poorly defined, and show overlapping phenotypes [83]. The most widely accepted population of pro-tumorigenic BMDCs are myeloid-derived suppressor cells (MDSCs), expressing both CD11b (a myeloid cell marker) and Gr1 (a granulocyte marker). MDSCs were originally investigated for their roles in suppressing $CD8^+$ T cell immunity, contributing to tumor escape from the host immune-surveillance [84–86]. Yang et al. demonstrated that $CD11b^+Gr1^+$ MDSCs promote vascular density and vascular maturation while decreasing necrosis [87, 88]. In addition, the authors showed that MDSCs express high levels of matrix metalloproteinase (MMP)-9, and also MDSCs acquire endothelial properties to incorporate into endothelium. Similarly, Kim et al. demonstrated that circulating monocytes in tumor-bearing hosts express an endothelial cell marker (CD31) and directly contribute to tumor angiogenesis [89]. However, the idea that MDSCs can differentiate into endothelial cells remains controversial and to be further investigated [90]. Interestingly, while tumors cannot grow in MMP-9 knockout mice, wild-type bone marrow transplantation can restore tumor growth in the same host, suggesting that BMDCs are the primary source of MMP-9 in tumor angiogenesis. $CD11b^+$ myeloid cells, but not endothelial progenitor cells, are the main source of MMP-9 in the tumor tissue [91], which can increase the bioavailability of VEGF and other endothelial growth factors. In addition, neutrophils have been shown to secrete VEGF [92]. Recent data from Yang et al. suggest that MDSCs enhance tumor cell invasion and contribute to TGF-β-mediated breast cancer metastasis [93]. Furthermore, recruitment of $CD11b^+Gr1^+$ cells is mediated by the two chemokine axes, SDF-1/CXCR4 and CXCL5/CXCR2 [93].

Given the roles of MDSCs in tumor angiogenesis and invasion, it is likely that MDSCs promote tumor growth and/or metastasis in any organ site including bone. In addition, the surface markers of MDSCs overlap with those of osteoclast lineage cells, suggesting that MDSCs have potential to differentiate into osteoclasts. However, the role of MDSCs specifically in bone metastasis is not yet clearly understood. Some supporting evidence came from the work of Mundy and colleagues who discovered that MDSCs were increased in the bone marrow and spleen in a syngeneic myeloma mouse model, and the MDSCs from the myeloma-bearing mice had a greater capacity to form osteoclasts, compared to the MDSCs from control mice [88, 94]. Furthermore, these authors presented their preliminary data that MDSCs can be precursors of osteoclasts in myeloma bone lesions [95], and also that an osteoclast inhibitor, zoledronic acid, suppressed the differentiation of MDSCs into osteoclasts [96].

Discussion and Conclusions

Bone marrow is comprised of diverse populations of hematopoietic lineage cells as well as stromal cells. Increasing lines of evidence support pro-tumorigenic roles of individual bone marrow-derived cell populations in such processes as angiogenesis, tumor cell apoptosis, escape from immune-surveillance, etc. However, each cell population mediates distinct and sometimes contradictory (pro- or anti-tumorigenic) roles, and continued research endeavors are required to delineate the complexity. This review article summarized key evidence describing the differential roles of hematopoietic lineage cells, including HSCs, megakaryocytes, macrophages and MDSCs in bone metastasis (see Fig. 1 for a schematic summary of data). Briefly, expansion of bone marrow cellularity has been found to promote prostate cancer skeletal metastasis, suggesting in general that cells in the bone marrow have tumorigenic functions [42]. Indeed, HSCs switch on angiogenesis, promoting tumor growth and potentially metastasis [41]. However, recent data demonstrated

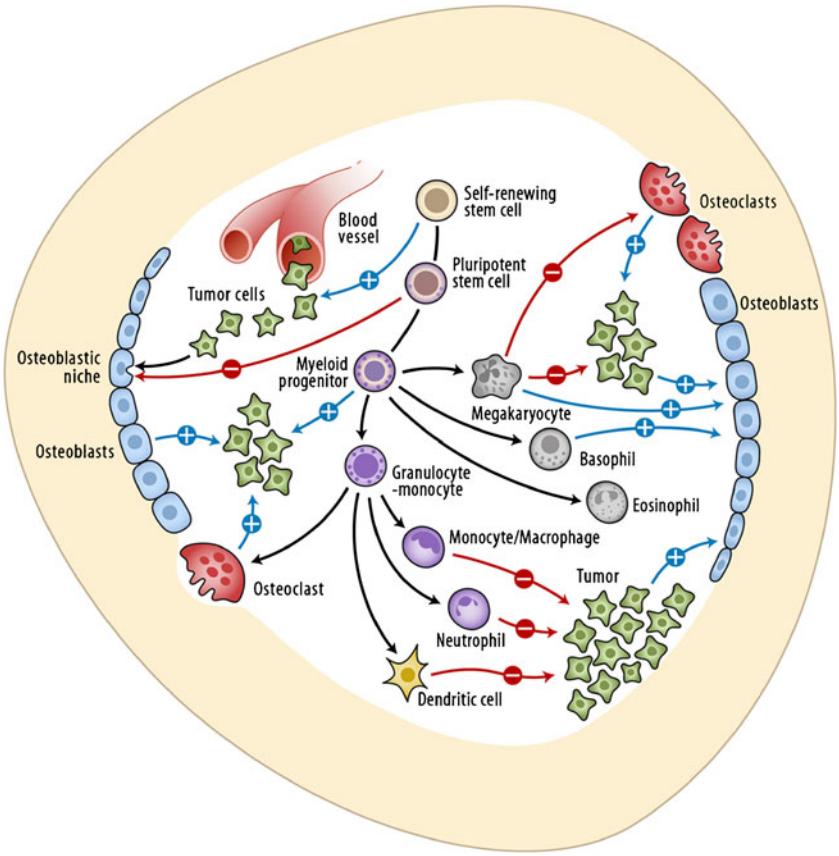

Fig. 1 Interactions between metastatic tumor cells and bone marrow cells are illustrated. Hematopoietic stem cells increase tumor growth by promoting angiogenesis and osteoblastogenesis. Concurrently, hematopoietic stem cells compete with metastatic tumor cells for occupancy of the osteoblastic niche, resulting in negative regulation of skeletal metastasis. Osteoblasts and osteoclasts both contribute to the positive feedback leading to tumor growth in bone (a 'vicious cycle'). Immune cells (phagocytic cells and dendritic cells) attack tumor cells. However, a subset of immune precursor cells (e.g. myeloid-derived suppressor cells) is implicated in promoting tumor growth and metastasis. Megakaryocytes induce apoptosis of extravasating tumor cells in bone, and also suppress tumor cell proliferation. (Legend: *blue arrows* with *circled plus mark* indicate positive regulation; *red arrows* with *circled minus mark* indicate negative regulation; and *black arrows* indicate differentiation. Cellular components of this cartoon are not proportionate to the actual size)

that tumor cells compete with HSCs for niche occupancy, thus the presence of HSCs can negatively regulate tumor metastasis to bone [40]. More interestingly, HSCs have been shown to increase bone morphogenetic proteins (BMP)-2 and 6 in response to erythropoietin stimuli, potentially contributing to augmented osteoblastogenesis [97]. These data collectively support that even a single cell population entity (i.e. HSCs) can have a dual function in the context of tumor metastasis to bone. For example, data demonstrate that mesenchymal stem cells (MSCs), which give rise to multiple types of stromal cells including adipocytes, muscles, fibroblasts, chondrocytes, etc., contribute to the creation of a favorable tumor microenvironment in general as well as in bone [23]. Contrarily, Naveiras et al. demonstrated that bone marrow adipocytes, which frequently infiltrate red marrow spaces after chemotherapy or radiation, negatively regulate HSCs [98].

Other components of the bone marrow such as megakaryocytes and macrophages also have unique roles in tumor progression. Megakaryocytes are potentially the first cells that extravasating tumor cells encounter in the bone marrow, and megakaryocytes induce tumor cell apoptosis and decreased proliferation [44]. Despite the lack of definitive experimental results in bone metastasis, macrophages, particularly TAMs, are highly likely to play critical roles in tumor growth and angiogenesis in bone. Similarly, MDSCs are essential components for a favorable tumor microenvironment. Collectively, as the bone marrow is the primary supplying organ of macrophages, monocytes and other immune cells, precursors and the differentiated macrophages and MDSCs surely play essential roles in bone metastasis.

Even with the data described in this article, elucidating the roles of bone marrow cells in the metastatic bone microenvironment remain a rich area of research opportunity. For example, one emerging question is how solid tumors in a primary organ site or in circulation regulate bone marrow cells before the occurrence of bone metastasis. The tumor microenvironment is comprised of primary tumor cells mixed

with multiple types of stromal cells, of which a significant fraction originates from the bone marrow. Increasing evidence supports the critical roles of those bone marrow-derived cells (BMDCs) in tumor progression. As BMDCs are such critical components, it is likely that primary tumors somehow communicate with the cells in the bone marrow to supply the indispensable components to enhance metastatic capacity. In addition, the data demonstrating that tumor cells prime the metastatic soil (termed 'pre-metastatic niche') before arrival of tumor cells in the metastatic recipient organ by VEGF-receptor 1-positive bone marrow cells [99, 100], suggest similar mechanisms may occur in the bone marrow before arrival of breast or prostate cancer cells in the bone marrow. Particularly, the unique bone-tropism of metastatic prostate or breast cancer cells may be due to breast or prostate tumor-derived factors modulating bone and bone marrow cells. One potential candidate molecule mediating crosstalk between tumor cells and bone marrow cells is parathyroid hormone-related peptide (PTHrP). PTHrP was first discovered as an etiologic factor for malignancy-induced hypercalcemia, and was later implicated in pro-tumorigenic roles such as cellular proliferation, angiogenesis as well as stimulating osteoblasts and osteoclasts. Similar to parathyroid hormone (PTH), a physiological counterpart, PTHrP promotes bone turnover and anabolic response, which can promote tumor growth in bone. In addition, PTHrP up-regulates cytokine expression from the bone marrow stromal cells (i.e. osteoblasts), including VEGF, IL-6 and C-C chemokine ligand (CCL)-2 (also known as monocyte chemoattractant protein [MCP]-1) all of which have the potential to promote bone marrow cells. Therefore, tumor cells in their primary organ site may secrete PTHrP to prime the cells in the bone marrow indirectly via up-regulating cytokines from osteoblasts, leading to expansion and/or potentiation of fractions of bone marrow cells (e.g. MDSCs). In turn, the primed bone marrow cells either cultivate the metastatic recipient site, and/or travel back to the primary tumor tissue to promote growth, invasion and angiogenesis. However, there is currently no data supporting this potential loop of crosstalk between tumor tissue and the bone marrow. Continued research in this field may yield potential mechanisms that could be targeted for the treatment and prevention of metastasis, thereby providing a means to increase length and quality of life for cancer patients.

Acknowledgements This work was financially supported by the Department of Defense Prostate Cancer Research Program Grants W81XWH-10-1-0546 (Serk In Park) and W81XWH-08-1-0037 (Laurie K. McCauley); and the National Cancer Institute Program Project Grant P01CA093900 (Laurie K. McCauley). The authors thank Janice E. Berry, Amy J. Koh and Matthew Eber for their assistance with preparation of this manuscript.

Conflict of Interest The authors declare no financial conflict of interest.

References

1. Fidler IJ (2003) The pathogenesis of cancer metastasis: the 'seed and soil' hypothesis revisited. Nat Rev Canc 3(6):453–458
2. Talmadge JE, Fidler IJ (2010) AACR centennial series: the biology of cancer metastasis: historical perspective. Canc Res 70 (14):5649–5669. doi:10.1158/0008-5472.CAN-10-1040
3. Fidler IJ (2002) Critical determinants of metastasis. Semin Canc Biol 12(2):89–96. doi:10.1006/scbi.2001.0416
4. Paget S (1989) The distribution of secondary growths in cancer of the breast. 1889. Canc Metastasis Rev 8(2):98–101
5. Ewing J (1928) Neoplastic diseases; a treatise on tumors. 3d ed rev. and enl., with 546 illustrations. edn. W.B. Saunders, Philadelphia, London
6. Geldof AA (1997) Models for cancer skeletal metastasis: a reappraisal of Batson's plexus. Anticancer Res 17(3A):1535–1539
7. Fidler IJ, Kripke ML (1977) Metastasis results from preexisting variant cells within a malignant tumor. Science 197(4306):893–895
8. Hart IR, Fidler IJ (1980) Role of organ selectivity in the determination of metastatic patterns of B16 melanoma. Canc Res 40(7):2281–2287
9. Tarin D, Price JE, Kettlewell MG, Souter RG, Vass AC, Crossley B (1984) Clinicopathological observations on metastasis in man studied in patients treated with peritoneovenous shunts. Br Med J (Clin Res Ed) 288(6419):749–751
10. Tarin D, Price JE, Kettlewell MG, Souter RG, Vass AC, Crossley B (1984) Mechanisms of human tumor metastasis studied in patients with peritoneovenous shunts. Canc Res 44 (8):3584–3592
11. Hess KR, Varadhachary GR, Taylor SH, Wei W, Raber MN, Lenzi R, Abbruzzese JL (2006) Metastatic patterns in adenocarcinoma. Cancer 106(7):1624–1633. doi:10.1002/cncr.21778
12. Bubendorf L, Schopfer A, Wagner U, Sauter G, Moch H, Willi N, Gasser TC, Mihatsch MJ (2000) Metastatic patterns of prostate cancer: an autopsy study of 1,589 patients. Hum Pathol 31(5):578–583
13. Mundy GR (2002) Metastasis to bone: causes, consequences and therapeutic opportunities. Nat Rev Canc 2(8):584–593. doi:10.1038/nrc867
14. Roodman GD (2004) Mechanisms of bone metastasis. New Engl J Med 350(16):1655–1664. doi:10.1056/NEJMra030831
15. Rubin MA, Putzi M, Mucci N, Smith DC, Wojno K, Korenchuk S, Pienta KJ (2000) Rapid ("warm") autopsy study for procurement of metastatic prostate cancer. Clin Canc Res 6 (3):1038–1045
16. Weilbaecher KN, Guise TA, McCauley LK (2011) Cancer to bone: a fatal attraction. Nat Rev Canc 11(6):411–425. doi:10.1038/nrc3055
17. Casimiro S, Guise TA, Chirgwin J (2009) The critical role of the bone microenvironment in cancer metastases. Mol Cell Endocrinol 310(1–2):71–81. doi:10.1016/j.mce.2009.07.004
18. Guise TA, Yin JJ, Taylor SD, Kumagai Y, Dallas M, Boyce BF, Yoneda T, Mundy GR (1996) Evidence for a causal role of parathyroid hormone-related protein in the pathogenesis of human breast cancer-mediated osteolysis. J Clin Investig 98 (7):1544–1549. doi:10.1172/JCI118947
19. Yin JJ, Selander K, Chirgwin JM, Dallas M, Grubbs BG, Wieser R, Massague J, Mundy GR, Guise TA (1999) TGF-beta signaling blockade inhibits PTHrP secretion by breast cancer cells and bone metastases development. J Clin Investig 103(2):197–206. doi:10.1172/JCI3523
20. Li X, Loberg R, Liao J, Ying C, Snyder LA, Pienta KJ, McCauley LK (2009) A destructive cascade mediated by CCL2 facilitates prostate cancer growth in bone. Canc Res 69(4):1685–1692. doi:10.1158/0008-5472.CAN-08-2164

21. Liao J, Li X, Koh AJ, Berry JE, Thudi N, Rosol TJ, Pienta KJ, McCauley LK (2008) Tumor expressed PTHrP facilitates prostate cancer-induced osteoblastic lesions. Int J Canc 123 (10):2267–2278. doi:10.1002/ijc.23602
22. Liao J, McCauley LK (2006) Skeletal metastasis: established and emerging roles of parathyroid hormone related protein (PTHrP). Canc Metastasis Rev 25(4):559–571. doi:10.1007/s10555-006-9033-z
23. Bergfeld SA, DeClerck YA (2010) Bone marrow-derived mesenchymal stem cells and the tumor microenvironment. Canc Metastasis Rev 29(2):249–261. doi:10.1007/s10555-010-9222-7
24. Ara T, Declerck YA (2010) Interleukin-6 in bone metastasis and cancer progression. Eur J Canc 46(7):1223–1231. doi:10.1016/j.ejca.2010.02.026
25. Paul WE (1999) Fundamental immunology, 4th edn. Lippincott-Raven, Philadelphia
26. Schermer S (1967) The blood morphology of laboratory animals, 3rd edn. Davis, Philadelphia
27. Travlos GS (2006) Normal structure, function, and histology of the bone marrow. Toxicol Pathol 34(5):548–565. doi:10.1080/01926230600939856
28. Shirota T, Tavassoli M (1991) Cyclophosphamide-induced alterations of bone marrow endothelium: implications in homing of marrow cells after transplantation. Exp Hematol 19(5):369–373
29. Shirota T, Tavassoli M (1992) Alterations of bone marrow sinus endothelium induced by ionizing irradiation: implications in the homing of intravenously transplanted marrow cells. Blood Cell 18(2):197–214
30. Weiss L, Geduldig U (1991) Barrier cells: stromal regulation of hematopoiesis and blood cell release in normal and stressed murine bone marrow. Blood 78(4):975–990
31. Tavassoli M, Hardy CL (1990) Molecular basis of homing of intravenously transplanted stem cells to the marrow. Blood 76 (6):1059–1070
32. Mazo IB, Gutierrez-Ramos JC, Frenette PS, Hynes RO, Wagner DD, von Andrian UH (1998) Hematopoietic progenitor cell rolling in bone marrow microvessels: parallel contributions by endothelial selectins and vascular cell adhesion molecule 1. J Exp Med 188(3):465–474
33. Frenette PS, Subbarao S, Mazo IB, von Andrian UH, Wagner DD (1998) Endothelial selectins and vascular cell adhesion molecule-1 promote hematopoietic progenitor homing to bone marrow. Proc Natl Acad Sci U S A 95(24):14423–14428
34. Peled A, Petit I, Kollet O, Magid M, Ponomaryov T, Byk T, Nagler A, Ben-Hur H, Many A, Shultz L, Lider O, Alon R, Zipori D, Lapidot T (1999) Dependence of human stem cell engraftment and repopulation of NOD/SCID mice on CXCR4. Science 283(5403):845–848
35. Muller A, Homey B, Soto H, Ge N, Catron D, Buchanan ME, McClanahan T, Murphy E, Yuan W, Wagner SN, Barrera JL, Mohar A, Verastegui E, Zlotnik A (2001) Involvement of chemokine receptors in breast cancer metastasis. Nature 410(6824):50–56. doi:10.1038/35065016
36. Taichman RS, Cooper C, Keller ET, Pienta KJ, Taichman NS, McCauley LK (2002) Use of the stromal cell-derived factor-1/CXCR4 pathway in prostate cancer metastasis to bone. Canc Res 62(6):1832–1837
37. Sun X, Cheng G, Hao M, Zheng J, Zhou X, Zhang J, Taichman RS, Pienta KJ, Wang J (2010) CXCL12/CXCR4/CXCR7 chemokine axis and cancer progression. Canc Metastasis Rev 29(4):709–722. doi:10.1007/s10555-010-9256-x
38. Jung Y, Wang J, Song J, Shiozawa Y, Havens A, Wang Z, Sun YX, Emerson SG, Krebsbach PH, Taichman RS (2007) Annexin II expressed by osteoblasts and endothelial cells regulates stem cell adhesion, homing, and engraftment following transplantation. Blood 110(1):82–90. doi:10.1182/blood-2006-05-021352
39. Shiozawa Y, Havens AM, Jung Y, Ziegler AM, Pedersen EA, Wang J, Lu G, Roodman GD, Loberg RD, Pienta KJ, Taichman RS (2008) Annexin II/annexin II receptor axis regulates adhesion, migration, homing, and growth of prostate cancer. J Cell Biochem 105(2):370–380. doi:10.1002/jcb.21835
40. Shiozawa Y, Pedersen EA, Havens AM, Jung Y, Mishra A, Joseph J, Kim JK, Patel LR, Ying C, Ziegler AM, Pienta MJ, Song J, Wang J, Loberg RD, Krebsbach PH, Pienta KJ, Taichman RS (2011) Human prostate cancer metastases target the hematopoietic stem cell niche to establish footholds in mouse bone marrow. J Clin Investig. doi:10.1172/JCI43414
41. Okamoto R, Ueno M, Yamada Y, Takahashi N, Sano H, Suda T, Takakura N (2005) Hematopoietic cells regulate the angiogenic switch during tumorigenesis. Blood 105(7):2757–2763. doi:10.1182/blood-2004-08-3317
42. Schneider A, Kalikin LM, Mattos AC, Keller ET, Allen MJ, Pienta KJ, McCauley LK (2005) Bone turnover mediates preferential localization of prostate cancer in the skeleton. Endocrinology 146(4):1727–1736. doi:10.1210/en.2004-1211
43. Lichtman MA, Chamberlain JK, Simon W, Santillo PA (1978) Parasinusoidal location of megakaryocytes in marrow: a determinant of platelet release. Am J Hematol 4(4):303–312
44. Li X, Koh AJ, Wang Z, Soki FN, Park SI, Pienta KJ, McCauley LK (2011) Inhibitory effects of megakaryocytic cells in prostate cancer skeletal metastasis. J Bone Miner Res 26(1):125–134. doi:10.1002/jbmr.204
45. Kacena MA, Gundberg CM, Horowitz MC (2006) A reciprocal regulatory interaction between megakaryocytes, bone cells, and hematopoietic stem cells. Bone 39(5):978–984. doi:10.1016/j.bone.2006.05.019
46. Kacena MA, Nelson T, Clough ME, Lee SK, Lorenzo JA, Gundberg CM, Horowitz MC (2006) Megakaryocyte-mediated inhibition of osteoclast development. Bone 39(5):991–999. doi:10.1016/j.bone.2006.05.004
47. Kacena MA, Shivdasani RA, Wilson K, Xi Y, Troiano N, Nazarian A, Gundberg CM, Bouxsein ML, Lorenzo JA, Horowitz MC (2004) Megakaryocyte-osteoblast interaction revealed in mice deficient in transcription factors GATA-1 and NF-E2. J Bone Miner Res 19 (4):652–660. doi:10.1359/JBMR.0301254
48. Bord S, Frith E, Ireland DC, Scott MA, Craig JI, Compston JE (2005) Megakaryocytes modulate osteoblast synthesis of type-1 collagen, osteoprotegerin, and RANKL. Bone 36(5):812–819. doi:10.1016/j.bone.2004.12.006
49. Calvi LM, Adams GB, Weibrecht KW, Weber JM, Olson DP, Knight MC, Martin RP, Schipani E, Divieti P, Bringhurst FR, Milner LA, Kronenberg HM, Scadden DT (2003) Osteoblastic cells regulate the haematopoietic stem cell niche. Nature 425 (6960):841–846. doi:10.1038/nature02040
50. Udagawa N, Takahashi N, Jimi E, Matsuzaki K, Tsurukai T, Itoh K, Nakagawa N, Yasuda H, Goto M, Tsuda E, Higashio K, Gillespie MT, Martin TJ, Suda T (1999) Osteoblasts/stromal cells stimulate osteoclast activation through expression of osteoclast differentiation factor/RANKL but not macrophage colony-stimulating factor: receptor activator of NF-kappa B ligand. Bone 25(5):517–523
51. Ahmed N, Khokher MA, Hassan HT (1999) Cytokine-induced expansion of human CD34+ stem/progenitor and CD34 + CD41 + early megakaryocytic marrow cells cultured on normal osteoblasts. Stem Cell 17(2):92–99. doi:10.1002/stem.170092
52. Roato I, D'Amelio P, Gorassini E, Grimaldi A, Bonello L, Fiori C, Delsedime L, Tizzani A, De Libero A, Isaia G, Ferracini R (2008) Osteoclasts are active in bone forming metastases of prostate cancer patients. PLoS One 3(11):e3627. doi:10.1371/journal.pone.0003627
53. Carmeliet P, Jain RK (2011) Molecular mechanisms and clinical applications of angiogenesis. Nature 473(7347):298–307. doi:10.1038/nature10144

54. Nieswandt B, Hafner M, Echtenacher B, Mannel DN (1999) Lysis of tumor cells by natural killer cells in mice is impeded by platelets. Canc Res 59(6):1295–1300
55. Boucharaba A, Serre CM, Gres S, Saulnier-Blache JS, Bordet JC, Guglielmi J, Clezardin P, Peyruchaud O (2004) Platelet-derived lysophosphatidic acid supports the progression of osteolytic bone metastases in breast cancer. J Clin Investig 114 (12):1714–1725. doi:10.1172/JCI22123
56. Gupta GP, Massague J (2004) Platelets and metastasis revisited: a novel fatty link. J Clin Investig 114(12):1691–1693. doi:10.1172/JCI23823
57. Mizutani K, Sud S, McGregor NA, Martinovski G, Rice BT, Craig MJ, Varsos ZS, Roca H, Pienta KJ (2009) The chemokine CCL2 increases prostate tumor growth and bone metastasis through macrophage and osteoclast recruitment. Neoplasia 11 (11):1235–1242
58. Loberg RD, Ying C, Craig M, Yan L, Snyder LA, Pienta KJ (2007) CCL2 as an important mediator of prostate cancer growth in vivo through the regulation of macrophage infiltration. Neoplasia 9 (7):556–562
59. Halin S, Rudolfsson SH, Van Rooijen N, Bergh A (2009) Extratumoral macrophages promote tumor and vascular growth in an orthotopic rat prostate tumor model. Neoplasia 11(2):177–186
60. Solinas G, Germano G, Mantovani A, Allavena P (2009) Tumor-associated macrophages (TAM) as major players of the cancer-related inflammation. J Leukoc Biol 86(5):1065–1073. doi:10.1189/jlb.0609385
61. Hiraoka K, Zenmyo M, Watari K, Iguchi H, Fotovati A, Kimura YN, Hosoi F, Shoda T, Nagata K, Osada H, Ono M, Kuwano M (2008) Inhibition of bone and muscle metastases of lung cancer cells by a decrease in the number of monocytes/macrophages. Canc Sci 99(8):1595–1602. doi:10.1111/j.1349-7006.2008.00880.x
62. Bingle L, Brown NJ, Lewis CE (2002) The role of tumour-associated macrophages in tumour progression: implications for new anticancer therapies. J Pathol 196(3):254–265. doi:10.1002/path.1027
63. Sica A, Larghi P, Mancino A, Rubino L, Porta C, Totaro MG, Rimoldi M, Biswas SK, Allavena P, Mantovani A (2008) Macrophage polarization in tumour progression. Semin Canc Biol 18(5):349–355. doi:10.1016/j.semcancer.2008.03.004
64. Balkwill F, Mantovani A (2001) Inflammation and cancer: back to Virchow? Lancet 357(9255):539–545. doi:10.1016/S0140-6736(00)04046-0
65. Loberg RD, Ying C, Craig M, Day LL, Sargent E, Neeley C, Wojno K, Snyder LA, Yan L, Pienta KJ (2007) Targeting CCL2 with systemic delivery of neutralizing antibodies induces prostate cancer tumor regression in vivo. Canc Res 67 (19):9417–9424. doi:10.1158/0008-5472.CAN-07-1286
66. Roca H, Varsos Z, Pienta KJ (2008) CCL2 protects prostate cancer PC3 cells from autophagic death via phosphatidylinositol 3-kinase/AKT-dependent survivin up-regulation. J Biol Chem 283(36):25057–25073. doi:10.1074/jbc.M801073200
67. Roca H, Varsos ZS, Sud S, Craig MJ, Ying C, Pienta KJ (2009) CCL2 and interleukin-6 promote survival of human CD11b + peripheral blood mononuclear cells and induce M2-type macrophage polarization. J Biol Chem 284(49):34342–34354. doi:10.1074/jbc.M109.042671
68. Zhang J, Lu Y, Pienta KJ (2010) Multiple roles of chemokine (C-C motif) ligand 2 in promoting prostate cancer growth. J Natl Canc Inst 102(8):522–528. doi:10.1093/jnci/djq044
69. Lin EY, Li JF, Gnatovskiy L, Deng Y, Zhu L, Grzesik DA, Qian H, Xue XN, Pollard JW (2006) Macrophages regulate the angiogenic switch in a mouse model of breast cancer. Canc Res 66(23):11238–11246. doi:10.1158/0008-5472.CAN-06-1278
70. Leek RD, Lewis CE, Whitehouse R, Greenall M, Clarke J, Harris AL (1996) Association of macrophage infiltration with angiogenesis and prognosis in invasive breast carcinoma. Canc Res 56(20):4625–4629
71. Hildenbrand R, Dilger I, Horlin A, Stutte HJ (1995) Urokinase and macrophages in tumour angiogenesis. Br J Canc 72(4):818–823
72. Miles DW, Happerfield LC, Naylor MS, Bobrow LG, Rubens RD, Balkwill FR (1994) Expression of tumour necrosis factor (TNF alpha) and its receptors in benign and malignant breast tissue. Int J Canc 56(6):777–782
73. Jung YJ, Isaacs JS, Lee S, Trepel J, Neckers L (2003) IL-1beta-mediated up-regulation of HIF-1alpha via an NFkappaB/COX-2 pathway identifies HIF-1 as a critical link between inflammation and oncogenesis. FASEB J 17(14):2115–2117. doi:10.1096/fj.03-0329fje
74. MacMicking J, Xie QW, Nathan C (1997) Nitric oxide and macrophage function. Annu Rev Immunol 15:323–350. doi:10.1146/annurev.immunol.15.1.323
75. Pollard JW (2004) Tumour-educated macrophages promote tumour progression and metastasis. Nat Rev Canc 4(1):71–78. doi:10.1038/nrc1256
76. Qian BZ, Pollard JW (2010) Macrophage diversity enhances tumor progression and metastasis. Cell 141(1):39–51. doi:10.1016/j.cell.2010.03.014
77. Lewis CE, Pollard JW (2006) Distinct role of macrophages in different tumor microenvironments. Canc Res 66(2):605–612. doi:10.1158/0008-5472.CAN-05-4005
78. Alexander K, Chang M, Maylin E, Kohler T, Muller R, Wu A, Van Rooijen N, Sweet M, Hume D, Raggatt L, Pettit A (2011) Osteal macrophages promote in vivo intramembranous bone healing in a mouse tibial injury model. J Bone Miner Res 26 (7):1517–1532. doi:10.1002/jbmr.354
79. Chang MK, Raggatt LJ, Alexander KA, Kuliwaba JS, Fazzalari NL, Schroder K, Maylin ER, Ripoll VM, Hume DA, Pettit AR (2008) Osteal tissue macrophages are intercalated throughout human and mouse bone lining tissues and regulate osteoblast function in vitro and in vivo. J Immunol 181(2):1232–1244
80. Dvorak HF (1986) Tumors: wounds that do not heal. Similarities between tumor stroma generation and wound healing. New Engl J Med 315(26):1650–1659. doi:10.1056/NEJM198612253152606
81. Zumsteg A, Christofori G (2009) Corrupt policemen: inflammatory cells promote tumor angiogenesis. Curr Opin Oncol 21(1):60–70. doi:10.1097/CCO.0b013e32831bed7e
82. Murdoch C, Muthana M, Coffelt SB, Lewis CE (2008) The role of myeloid cells in the promotion of tumour angiogenesis. Nat Rev Canc 8(8):618–631. doi:10.1038/nrc2444
83. Coffelt SB, Lewis CE, Naldini L, Brown JM, Ferrara N, De Palma M (2010) Elusive identities and overlapping phenotypes of proangiogenic myeloid cells in tumors. Am J Pathol 176 (4):1564–1576. doi:10.2353/ajpath.2010.090786
84. Nagaraj S, Gupta K, Pisarev V, Kinarsky L, Sherman S, Kang L, Herber DL, Schneck J, Gabrilovich DI (2007) Altered recognition of antigen is a mechanism of CD8+ T cell tolerance in cancer. Nat Med 13(7):828–835. doi:10.1038/nm1609
85. Gabrilovich DI, Nagaraj S (2009) Myeloid-derived suppressor cells as regulators of the immune system. Nat Rev Immunol 9 (3):162–174. doi:10.1038/nri2506
86. Nagaraj S, Gabrilovich DI (2008) Tumor escape mechanism governed by myeloid-derived suppressor cells. Canc Res 68 (8):2561–2563. doi:10.1158/0008-5472.CAN-07-6229
87. Yang L, DeBusk LM, Fukuda K, Fingleton B, Green-Jarvis B, Shyr Y, Matrisian LM, Carbone DP, Lin PC (2004) Expansion of myeloid immune suppressor Gr + CD11b + cells in tumor-bearing host directly promotes tumor angiogenesis. Canc Cell 6 (4):409–421. doi:10.1016/j.ccr.2004.08.031
88. Yang L, Edwards CM, Mundy GR (2010) Gr-1 + CD11b + myeloid-derived suppressor cells (MDSCs): formidable partners in tumor

metastasis. J Bone Miner Res 25(8):1701–1706. doi:10.1002/jbmr.154
89. Kim SJ, Kim JS, Papadopoulos J, Wook Kim S, Maya M, Zhang F, He J, Fan D, Langley R, Fidler IJ (2009) Circulating monocytes expressing CD31: implications for acute and chronic angiogenesis. Am J Pathol 174(5):1972–1980. doi:10.2353/ajpath.2009.080819
90. Shojaei F, Zhong C, Wu X, Yu L, Ferrara N (2008) Role of myeloid cells in tumor angiogenesis and growth. Trends Cell Biol 18(8):372–378. doi:10.1016/j.tcb.2008.06.003
91. Ahn GO, Brown JM (2008) Matrix metalloproteinase-9 is required for tumor vasculogenesis but not for angiogenesis: role of bone marrow-derived myelomonocytic cells. Canc Cell 13 (3):193–205. doi:10.1016/j.ccr.2007.11.032
92. Taichman NS, Young S, Cruchley AT, Taylor P, Paleolog E (1997) Human neutrophils secrete vascular endothelial growth factor. J Leukoc Biol 62(3):397–400
93. Yang L, Huang J, Ren X, Gorska AE, Chytil A, Aakre M, Carbone DP, Matrisian LM, Richmond A, Lin PC, Moses HL (2008) Abrogation of TGF beta signaling in mammary carcinomas recruits Gr-1 + CD11b + myeloid cells that promote metastasis. Canc Cell 13(1):23–35. doi:10.1016/j.ccr.2007.12.004
94. ASBMR 29th Annual Meeting (2007) J Bone Miner Res 22(S1): s2–s51. doi:10.1002/jbmr.5650221402
95. Zhuang J, Yang L, Lwin ST, Edwards CM, Edwards JR, Mundy GR (2008) Osteoclasts in myeloma are derived from Gr-1 + CD11b + myeloid immune suppressor cells of the bone marrow niche in vivo. ASH Annu Meet Abstr 112(11):736
96. Melani C, Sangaletti S, Barazzetta FM, Werb Z, Colombo MP (2007) Amino-biphosphonate-mediated MMP-9 inhibition breaks the tumor-bone marrow axis responsible for myeloid-derived suppressor cell expansion and macrophage infiltration in tumor stroma. Canc Res 67(23):11438–11446. doi:10.1158/0008-5472.CAN-07-1882
97. Shiozawa Y, Jung Y, Ziegler AM, Pedersen EA, Wang J, Wang Z, Song J, Lee CH, Sud S, Pienta KJ, Krebsbach PH, Taichman RS (2010) Erythropoietin couples hematopoiesis with bone formation. PLoS One 5(5):e10853. doi:10.1371/journal.pone.0010853
98. Naveiras O, Nardi V, Wenzel PL, Hauschka PV, Fahey F, Daley GQ (2009) Bone-marrow adipocytes as negative regulators of the haematopoietic microenvironment. Nature 460(7252):259–263. doi:10.1038/nature08099
99. Kaplan RN, Psaila B, Lyden D (2006) Bone marrow cells in the 'pre-metastatic niche': within bone and beyond. Canc Metastasis Rev 25(4):521–529. doi:10.1007/s10555-006-9036-9
100. Kaplan RN, Riba RD, Zacharoulis S, Bramley AH, Vincent L, Costa C, MacDonald DD, Jin DK, Shido K, Kerns SA, Zhu Z, Hicklin D, Wu Y, Port JL, Altorki N, Port ER, Ruggero D, Shmelkov SV, Jensen KK, Rafii S, Lyden D (2005) VEGFR1-positive haematopoietic bone marrow progenitors initiate the pre-metastatic niche. Nature 438(7069):820–827. doi:10.1038/nature04186

Nuclear localization of parathyroid hormone-related peptide confers resistance to anoikis in prostate cancer cells

Serk In Park[1] *and Laurie K McCauley*[1,2]

[1]Department of Periodontics and Oral Medicine, University of Michigan School of Dentistry, 1011 North University Avenue, Ann Arbor, Michigan 48109, USA
[2]Department of Pathology, University of Michigan Medical School, 1500 East Medical Center Drive, Ann Arbor, Michigan 48109, USA

(Correspondence should be addressed to L K McCauley at Department of Periodontics and Oral Medicine, University of Michigan School of Dentistry; Email: mccauley@umich.edu)

Abstract

Prostate cancer remains a leading cause of cancer-related death in men, largely attributable to distant metastases, most frequently to bones. Despite intensive investigations, molecular mechanisms underlying metastasis are not completely understood. Among prostate cancer-derived factors, parathyroid hormone-related peptide (PTHrP), first discovered as an etiologic factor for malignancy-induced hypercalcemia, regulates many cellular functions critical to tumor growth, angiogenesis, and metastasis. In this study, the role of PTHrP in tumor cell survival from detachment-induced apoptosis (i.e. anoikis) was investigated. Reduction of *PTHLH* (encoding PTHrP) gene expression in human prostate cancer cells (PC-3) increased the percentage of apoptotic cells when cultured in suspension. Conversely, overexpression of PTHrP protected prostate cancer cells (Ace-1 and LNCaP, both typically expressing low or undetectable basal PTHrP) from anoikis. Overexpression of nuclear localization signal (NLS)-defective PTHrP failed to protect cells from anoikis, suggesting that PTHrP-dependent protection from anoikis is an intracrine event. A PCR-based apoptosis-related gene array showed that detachment increased expression of the *TNF* gene (encoding the proapoptotic protein tumor necrosis factor-α) fourfold greater in PTHrP-knockdown PC-3 cells than in control PC-3 cells. In parallel, *TNF* gene expression was significantly reduced in PTHrP-overexpressing LNCaP cells, but not in NLS-defective PTHrP overexpressing LNCaP cells, when compared with control LNCaP cells. Subsequently, in a prostate cancer skeletal metastasis mouse model, PTHrP-knockdown PC-3 cells resulted in significantly fewer metastatic lesions compared to control PC-3 cells, suggesting that PTHrP mediated antianoikis events in the bloodstream. In conclusion, nuclear localization of PTHrP confers prostate cancer cell resistance to anoikis, potentially contributing to prostate cancer metastasis.

Endocrine-Related Cancer (2012) **19** 1–12

Introduction

Prostate cancer is the second most frequently diagnosed cancer and the sixth leading cause of cancer-related death in males worldwide, notwithstanding the improved early detection methods and therapeutic modalities (Jemal *et al*. 2011). Advanced-stage prostate cancer patients commonly develop metastatic lesions, most frequently in the skeleton, which ultimately account for the high mortality rate as well as severe morbidities (Weilbaecher *et al*. 2011). In sharp contrast, the molecular mechanism leading to metastasis is not yet completely understood. Metastatic colonization in distant organs requires disseminating tumor cells to have essential cellular functions, such as invasion of extracellular matrices, survival in the bloodstream, extravasation, and

DOI: 10.1530/ERC-11-0278
1351–0088/12/019–001
Online version via http://www.endocrinology-journals.org

adaptation to the new environment (Langley & Fidler 2011), which are mediated by numerous tumor-derived factors. Prostate cancer is uniquely positioned because of its strong propensity to interact with and metastasize to bone. In this regard, prostate cancer cells express numerous bone-modulating cytokines including parathyroid hormone-related peptide (PTHrP), osteoprotegerin, receptor activator of nuclear factor-κB ligand, and others (Deftos *et al*. 2005). However, contributions of these bone-modulating factors to metastasis remain under investigation.

PTHrP was first discovered as an etiologic factor for malignancy-induced hypercalcemia by increasing osteoclastogenesis (Suva *et al*. 1987). Later, PTHrP expression was identified in carcinoma cells, such as lung, breast, and prostate cancer cells (Moseley *et al*. 1987, Iwamura *et al*. 1993, Downey *et al*. 1997). Similar to its physiologic counterpart, PTH, PTHrP binds to its cognate PTH/PTHrP receptor (PPR) expressed on osteoblasts and also found in some tumor cells (Downey *et al*. 1997, Iddon *et al*. 2000), triggering the cyclic AMP/protein kinase A signal transduction pathway. In addition to autocrine/paracrine effects mediated by receptor binding, PTHrP has been shown to localize to the nucleus, leading to the inhibition of apoptosis in chondrocytes and prostate cancer cells (Henderson *et al*. 1995, Dougherty *et al*. 1999). Chondrocytes expressing PTHrP with a deletion of the nuclear localization signal (NLS) showed increased apoptosis (Henderson *et al*. 1995), indicating that PTHrP functions as an antiapoptotic factor. However, the potential role of PTHrP in tumor cells, particularly in the context of metastatic cascades, is under investigation. For example, tumor cells are triggered to undergo apoptosis when the cells lose attachment to their extracellular matrix, a cellular phenomenon termed anoikis. Evasion of anoikis in the metastatic process (e.g. in the bloodstream) is essential for successful colonization of tumor cells in distant organs (Sakamoto & Kyprianou 2010).

In this study, the function of PTHrP in the context of prostate cancer was examined using an *in vitro* anoikis model as well as an *in vivo* experimental bone metastasis model. PTHrP protected prostate cancer cells from anoikis, effects of which were mediated by nuclear localization of PTHrP and reduced expression of tumor necrosis factor-α (TNF-α). Prostate tumor cells expressing lower PTHrP resulted in significantly fewer metastatic lesions compared to cells expressing higher PTHrP, potentially mediated by increased anoikis due to loss of intracrine PTHrP activity.

Materials and methods

Cells

PC-3, LNCaP, and Ace-1 prostate carcinoma cells were selected to study the function of PTHrP, because PC-3 cells express high levels of endogenous PTHrP while LNCaP and Ace-1 cells do not express detectable PTHrP. The canine prostate carcinoma cell line (Ace-1) was kindly provided by Dr Thomas Rosol (Ohio State University, USA; LeRoy *et al*. 2006, Thudi *et al*. 2011). Cells were maintained as monolayer cultures in RPMI-1640 media supplemented with 10% v/v fetal bovine serum and 1× penicillin/streptomycin and glutamate (all from Invitrogen). For *in vivo* bioluminescence imaging, luciferase-labeled PC-3 cells (designated PC-3^{Luc}) were produced by stably transfecting a luciferase-expressing pLazarus retroviral construct as previously described (Schneider *et al*. 2005). In addition, *PTHLH* (NCBI reference number: NM_198966) gene expression was reduced in PC-3^{Luc} cells via a lentiviral vector (pLenti4/Block-iT DEST vector; Invitrogen) expressing short hairpin RNA targeting 5′-GGGCAGATACCTAACTCAGGA-3′. An empty vector was used as a control. Lentiviral supernatants were prepared using 293T packaging cells (the University of Michigan Viral Vector Core Laboratory, Ann Arbor, MI, USA), followed by transduction of PC-3^{Luc} cells with polybrene (6 μg/ml). Subsequently, transduced cells were grown in bleomycin selection media (Zeocin 200 μg/ml; Invitrogen), and stable clones were selected and expanded for further experiments.

LNCaP and Ace-1 cells normally express undetectable basal levels of PTHrP. Both cell lines were stably transfected with full-length PTHrP, NLS-defective PTHrP (i.e. amino acids 87–107) (Henderson *et al*. 1995), or empty pcDNA3.1 vectors, as previously described (Dougherty *et al*. 1999, Liao *et al*. 2008).

Measurement of PTHrP

PTHrP expression was measured from the culture supernatant using an IRMA kit (Diagnostic Systems Laboratories, Webster, TX, USA), detecting amino acids 1–87 (Ratcliffe *et al*. 1991). Briefly, one million cells were seeded in a six-well plate in complete RPMI-1640 media (in triplicate), followed by media change with serum-free RPMI-1640 24 h later. Subsequently, cells were incubated for 48 h and cell-free supernatants collected. The PTHrP assay was performed as suggested by the manufacturer.

Calculation of *in vitro* doubling time

PTHrP-knockdown and empty vector control PC-3^{Luc} cells were synchronized (by overnight serum starvation), followed by seeding (1×10^5 cells/well, in triplicate) and enumeration at 24, 48, 72, and 96 h later with the aid of a hemacytometer and trypan blue dye. The doubling time (T_d) was calculated using the formula: $T_d=(T_2-T_1)\times(\log2/\log(Q_2/Q_1))$, where Q_1 and Q_2 are cell numbers at two time points (T_1 and T_2) respectively.

In vivo tumor growth

All animal experimental protocols were approved and performed in accordance with current regulations and standards of the University of Michigan's Institutional Animal Care and Use Committee guidelines.

For *in vivo* tumor growth, male athymic mice (Hsd: Athymic nude –*Foxn1*^{nu}; 4 weeks old; Harlan Laboratories, Indianapolis, IN, USA) were anesthetized and 100 µl of cell suspension containing 1×10^6 cells were mixed with 100 µl of growth factor reduced Matrigel (Invitrogen), and injected subcutaneously into both flanks ($n=10$ each group). After 3 weeks, bioluminescence imaging was performed to measure tumor size, followed by euthanasia and tumor tissue harvesting.

Anoikis assay and flow cytometry

To induce anoikis *in vitro*, prostate cancer cells were cultured in suspension as previously described (Minard *et al*. 2006). Briefly, six-well tissue culture plates were covered with 4% w/v endotoxin-free agarose. Prostate cancer cells were ~80% confluent at the initiation of overnight serum-starvation (for synchronization). Subsequently, cells were trypsinized and counted, followed by seeding of 1×10^6 cells/well in RMPI-1640 media supplemented with 2% v/v fetal bovine serum on regular culture plates or agarose-covered plates (in sextuplicate). After 12–16 h of incubation at 37 °C, cells were harvested by pipetting (for cells in suspension) or trypsinization (for attached cells), followed by washing with ice-cold PBS and centrifugation.

For flow cytometric analyses, cells were re-suspended in Annexin V binding buffer (BD Biosciences, San Jose, CA, USA), followed by addition of FITC-conjugated anti-Annexin V and propidium iodide (BD Biosciences). Subsequently, cells were washed once with ice-cold PBS and analyzed by flow cytometer (BD FACSCalibur) with CellQuest analyses software (BD Biosciences).

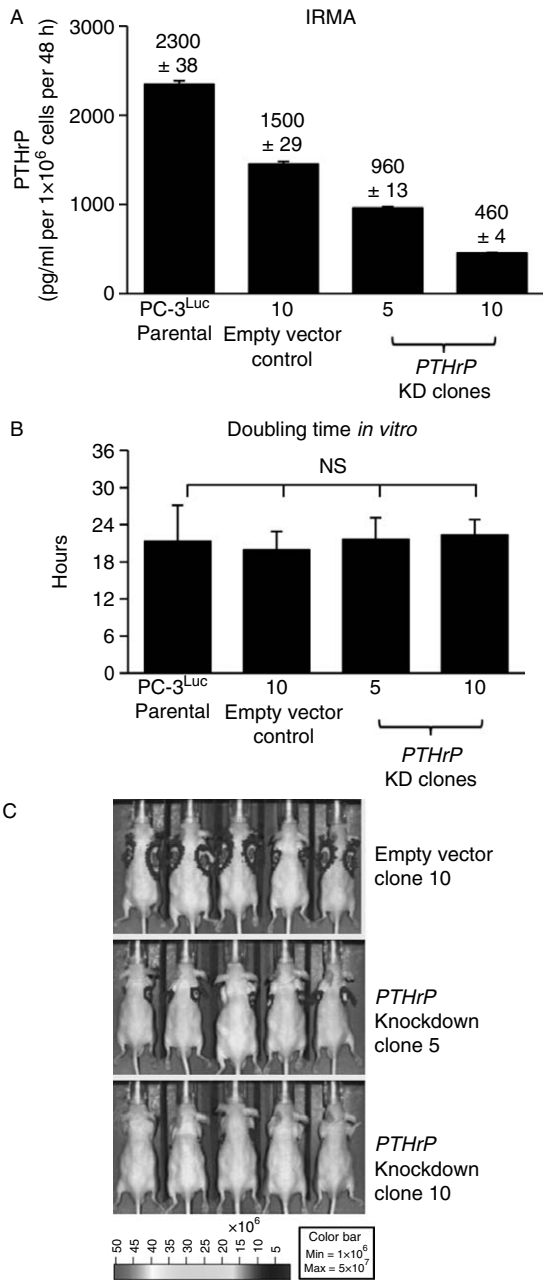

Figure 1 Generation of PC-3 prostate cancer cells expressing varying levels of PTHrP. PTHrP expression was reduced in PC-3^{Luc} cells via lentiviral shRNA. (A) PTHrP protein levels were measured from the culture supernatant by IRMA. Data are average of two measurements ±S.D. Assays were repeated more than three times, and one set of representative data is shown. (B) *In vitro* doubling time of the PC-3 clones expressing varying levels of PTHrP was calculated by enumeration of viable cells at 24, 48, 72, and 96 h time points ($n=3$ each). Data are mean±S.D. NS, not significant. (C) *In vivo* tumor size was measured by bioluminescence imaging. Subcutaneous tumors were grown for 20 days ($n=10$ per group). Five representative mice are shown. Tumor incidence was 100% in all three groups, determined by microscopic examination of tumor cells upon necropsy.

Apoptotic gene array

PTHrP-knockdown and empty vector control PC-3^{Luc} cells were grown on regular or 4% w/v agarose-covered 10 cm tissue culture plates (in duplicate) for 16 h. Subsequently, cells were lysed and total RNA was prepared (Qiagen RNeasy Mini Kit; Qiagen). RNA samples were reverse transcribed (RT^2 First Strand Kit; SA Biosciences, Frederick, MD, USA), followed by quantitative PCR-based human apoptotic gene array (SA Biosciences) according to the manufacturer's suggested protocols (Li *et al.* 2011). Analyses of data were performed using computer software provided by the manufacturer. A complete list of 84 apoptosis-related genes included in the analyses, detailed protocols, and analysis method can be found at the manufacturer's website (http://www.sabiosciences.com/rt_pcr_product/HTML/PAHS-012A.html).

In vivo metastasis model

To test the metastatic potentials of PC-3^{Luc} clones, cells were inoculated into the systemic circulation via intracardiac route, as previously described (Park *et al.* 2011*a*), followed by *in vivo* bioluminescence imaging. In brief, male athymic mice (Hsd: Athymic nude –*Foxn1*^{nu}; 6 weeks old; Harlan Laboratories) were anesthetized and 100 µl of cell suspension containing 2×10^5 cells were injected into the left heart ventricle. Systemic circulation of the tumor cells was confirmed by *in vivo* bioluminescence imaging immediately after inoculation. Metastatic hind limb tumors were detected and quantified by bioluminescence imaging (Caliper Life Sciences, Alameda, CA, USA). Tumor-bearing hind limb bones were harvested at euthanasia, fixed in 10% v/v buffered formaldehyde and decalcified in 10% w/v EDTA for 2 weeks. Metastatic tumor cells were microscopically confirmed.

Cytokines and antibodies

Recombinant human TNF-α and anti-human TNF-α neutralizing antibodies were purchased from Peprotech, Inc. (Rocky Hill, NJ, USA). For western blotting, anti-PTHrP antibody (H-137: a rabbit polyclonal antibody against amino acids 41–177 of human PTHrP) was purchased from Santa Cruz Biotechnology (Santa Cruz, CA, USA).

Statistical analyses

All statistical tests were performed by Microsoft Excel or GraphPad Prism Version 5 (La Jolla, CA,

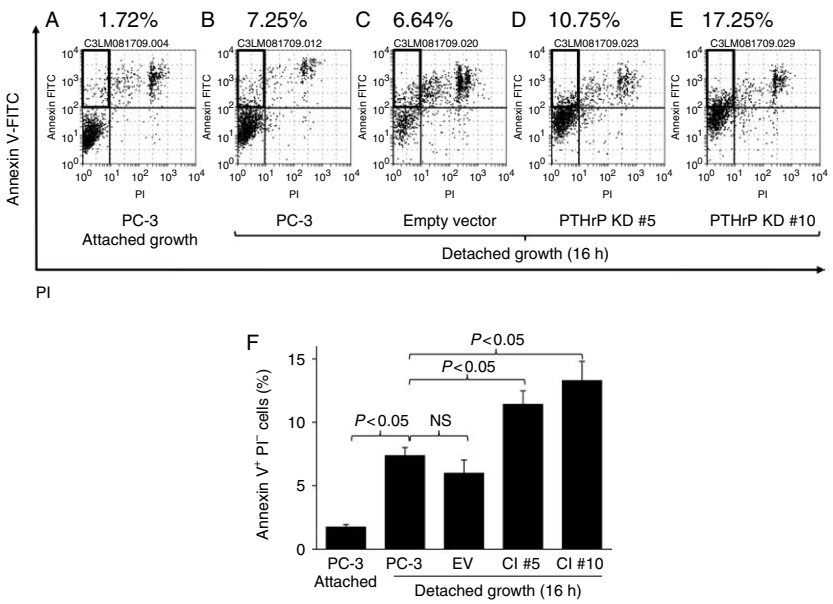

Figure 2 Reduction of PTHrP expression sensitized PC-3 cells to detachment-induced apoptosis. PC-3 cells expressing varying levels of PTHrP were induced to undergo anoikis, followed by flow cytometric analyses of apoptotic cells. Cells were seeded on regular six-well plates as a control, or on agarose-covered plates to induce anoikis ($n=6$ each). (A, B, C, D and E) Representative flow cytometric dot plots are shown. Annexin V^+PI^- cells (marked with boxes in the upper left quadrants) indicate apoptotic cells. (F) Average percentage of apoptotic cells is shown graphically. Data are mean ±S.D. $P<0.05$ by Student's *t*-test was considered statistically significant. NS, not significant.

USA). Student's *t*-test was used to compare two groups and the $P<0.05$ level was considered statistically significant. All statistical tests were two-sided and data expressed as a mean ± S.D.

Results

PTHrP-knockdown reduced *in vivo* tumor growth without affecting *in vitro* proliferation

As a first approach to investigate the function of PTHrP in prostate cancer cells, *PTHLH* gene expression was reduced in PC-3^{Luc} human prostate cancer cells using an shRNA technique. Stable clones were confirmed and selected according to level of PTHrP expression (Fig. 1A) in the cell culture supernatants. Two knockdown clones (clone no. 5 and 10) showed more than 50% reduction of PTHrP expression compared to parental PC-3^{Luc} cells, while an empty vector control clone also showed mild reduction, but not to the extent of clones 5 and 10. PTHrP has been shown to regulate cellular proliferation (Dougherty *et al*. 1999). However, cell enumeration assays demonstrated that PTHrP-knockdown did not affect *in vitro* cellular doubling time of PC-3^{Luc} cells (Fig. 1B), suggesting that the reduced level of PTHrP expression was sufficient to maintain cellular proliferation, at least in PC-3^{Luc} cells which express high basal levels of PTHrP. In contrast, PTHrP-knockdown resulted in significantly reduced tumor growth *in vivo* (Fig. 1C), suggesting that PTHrP regulates tumor cell proliferation and/or survival via a mechanism other than direct regulation of cell proliferation.

Reduction of PTHrP expression sensitized PC-3^{Luc} cells to detachment-induced apoptosis

In routine maintenance subculturing, differential plating efficiency among PTHrP-knockdown and control clones was noted, leading to a hypothesis that PTHrP-knockdown PC-3 cells are more prone to detachment-induced apoptosis. To test this, PC-3^{Luc} cells and PTHrP-knockdown clones were grown in suspension for an extended time, followed by flow cytometric analyses of apoptotic cells. Detachment increased the percentage of apoptotic Annexin V$^+$PI$^-$ PC-3^{Luc} cells (Fig. 2A and B), and empty vector control cells (Fig. 2C). Interestingly, PTHrP-knockdown clones had a significantly increased percentage of Annexin V$^+$PI$^-$ apoptotic cells (Fig. 2D, E and F),

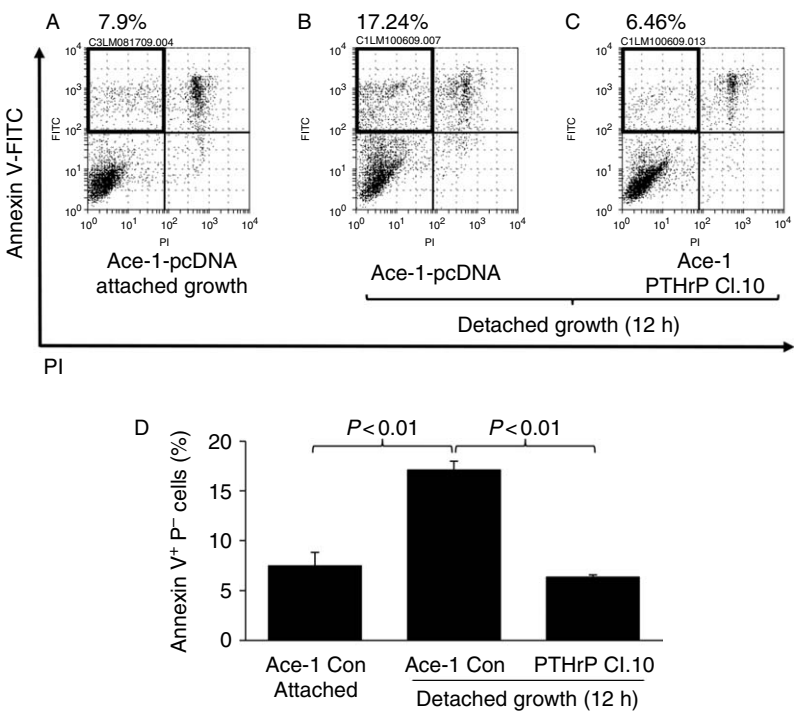

Figure 3 Ectopic expression of PTHrP rescued Ace-1 prostate cancer cells from anoikis. Ace-1 prostate cancer cells (expressing undetectable basal PTHrP) were engineered to express full-length PTHrP or control vector (pcDNA3.1), followed by anoikis assay. (A, B and C) Representative flow cytometric dot plots are shown. Annexin V$^+$PI$^-$ cells (marked with boxes in the upper left quadrants) indicate apoptotic cells. (D) Average percentage of apoptotic cells is shown graphically ($n=6$). Data are mean ± S.D. $P<0.05$ by Student's *t*-test was considered statistically significant.

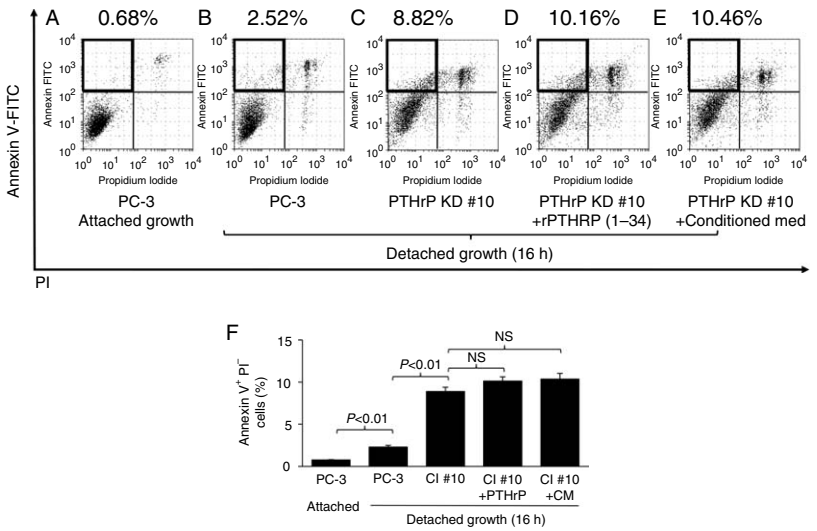

Figure 4 Exogenous PTHrP failed to rescue PC-3 cells from anoikis. PTHrP-knockdown PC-3 cells were induced to undergo anoikis in combination with recombinant PTHrP (1–34) or conditioned media from the PC-3 cell culture, followed by flow cytometric analyses of apoptotic cells. (A, B, C, D and E) Representative flow cytometric dot plots are shown. Annexin V^+PI^- cells (marked with boxes in the upper left quadrants) indicate apoptotic cells. (F) Average percentage of apoptotic cells is shown. Data are mean ± S.D. $P<0.05$ by Student's *t*-test was considered statistically significant. NS, not significant.

indicating that reduction of PTHrP expression inhibits survival of prostate tumor cells in suspension.

PTHrP overexpression rescued Ace-1 prostate cancer cells from anoikis

To further investigate the role of PTHrP in anoikis, an alternative approach (i.e. ectopic expression of PTHrP) was employed. An additional prostate cancer cell line, Ace-1, had been previously shown to express undetectable levels of PTHrP (Liao *et al*. 2008). A PTHrP overexpression vector or empty pcDNA3.1 vector (as a control) was transfected into Ace-1 cells, resulting in Ace-1 PTHrP clone 10 and Ace-1 pcDNA respectively. PTHrP expression was measured and confirmed by IRMA of culture supernatants. The Ace-1 PTHrP clone 10 expressed 282.2 ± 9.83 (pg/ml per 1×10^6 cells per 48 h), while Ace-1 pcDNA control cells expressed undetectable levels of PTHrP. Cells were induced to undergo anoikis by culturing in suspension (Fig. 3). PTHrP overexpressing Ace-1 cells had significantly fewer apoptotic cells compared to Ace-1 pcDNA control cells (Fig. 3A, B, C and D), indicating a causal role of PTHrP in protection from anoikis.

Recombinant PTHrP (1–34) failed to rescue PC-3 cells from anoikis

Data in Figs 2 and 3 demonstrated that prostate tumor cells expressing higher PTHrP have increased survival from detachment-induced apoptosis. Because PTHrP functions primarily via paracrine/autocrine manners through its cognate PTH type 1 receptor (PPR), we next tested whether exogenous PTHrP would rescue the PTHrP-knockdown clones from anoikis. Recombinant PTHrP (amino acids 1 through 34, the functional PPR-binding fragment) or conditioned media from the parental PC-3^{Luc} cell culture which contains full-length PTHrP was added to PTHrP-knockdown PC-3 clones in suspension. Neither recombinant PTHrP (1–34) nor the conditioned media rescued PTHrP-knockdown PC-3 cells from anoikis (Fig. 4), suggesting that PTHrP-dependent survival is not via N-terminus paracrine effects.

Overexpression of full-length PTHrP, but not NLS-defective PTHrP, rescues prostate cancer cells from anoikis

PTHrP localizes to the nucleus and has been shown to protect colon tumor cells from drug-induced apoptosis (Shen *et al*. 2007*a*, Bhatia *et al*. 2009*b*). This mechanism was evaluated on PTHrP- or NLS-defective PTHrP overexpressing prostate tumor cells. Human prostate cancer cells, LNCaP, expressing undetectable basal levels of PTHrP were engineered to express full-length PTHrP (designated PTHrP OE), NLS-defective PTHrP (designated PTHrP ΔNLS), or pcDNA3.1 (as a control) (Fig. 5G). Cells were cultured in suspension to induce anoikis, followed by flow cytometric analyses. Interestingly, NLS-defective PTHrP failed to rescue LNCaP

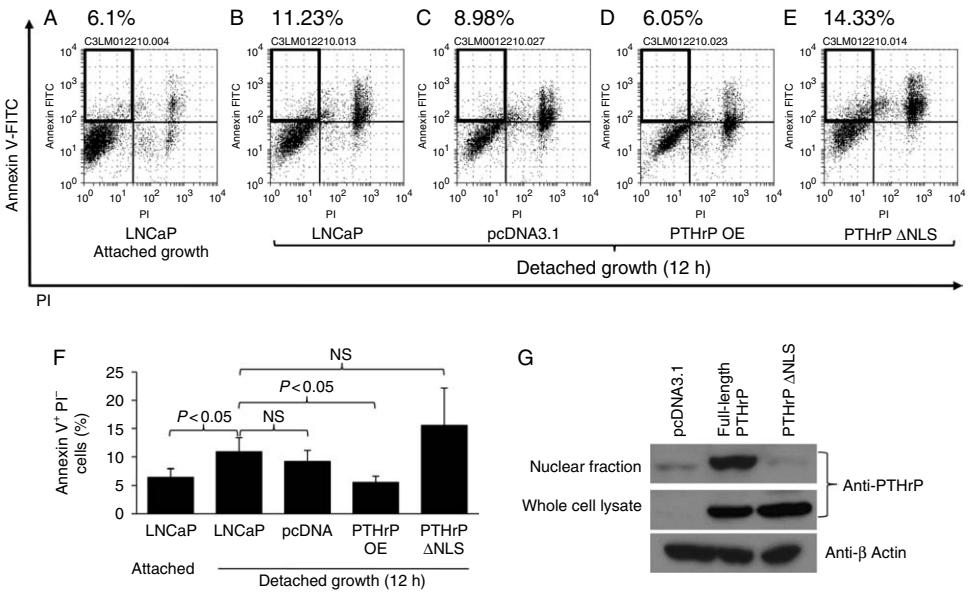

Figure 5 Full-length PTHrP, but not NLS-defective PTHrP, protected prostate cancer cells from anoikis. LNCaP prostate cancer cells were transfected with pcDNA 3.1 (control), PTHrP OE, or PTHrP ΔNLS, followed by anoikis assay. (A, B, C, D and E) Representative flow cytometric dot plots are shown. Annexin V^+PI^- cells (marked with boxes in the upper left quadrants) indicate apoptotic cells. (F) Average percentage of apoptotic cells is shown ($n=6$). Data are mean ± S.D. $P<0.05$ by Student's *t*-test was considered statistically significant. NS, not significant. (G) Western blotting analyses show high nuclear PTHrP in the PTHrP overexpressing clone and very low nuclear PTHrP in the PTHrP ΔNLS clone. Total cellular and nuclear lysates were prepared from the PTHrP OE, PTHrP ΔNLS, and pcDNA control cells, and PTHrP expression was detected by western blotting.

cells from anoikis, while full-length PTHrP significantly supported LNCaP cell survival in suspension (Fig. 5A, B, C, D, E and F). Overall, Figs 1, 2, 3, 4 and 5 demonstrate that PTHrP promotes prostate tumor cell survival from detachment-induced apoptosis via an intracrine manner (nuclear localization) and not a paracrine manner, potentially contributing to tumor growth *in vivo*.

Detachment induced greater TNF-α expression in PTHrP-knockdown PC-3 cells than in empty vector control cells

To investigate downstream mediators of PTHrP-dependent anoikis, a quantitative PCR-based gene array (detecting 84 human apoptosis-related genes) experiment was performed. Detachment-induced genes were identified by comparing mRNA from cells cultured in an agarose-covered plate with cells cultured on a regular plate (columns (A) and (B) in Table 1). Among 84 apoptosis-related genes tested, tumor necrosis factor-α (*TNF*) gene expression was increased more than fourfold in PTHrP-knockdown PC-3 cells compared to empty vector control PC-3 cells, indicating an inverse correlation of PTHrP nuclear localization with a proapoptotic gene (*TNF*).

NLS-defective PTHrP failed to decrease *TNF* in response to detachment

To validate the observation in the gene array data (Table 1), detachment-induced *TNF* expression was confirmed in an additional cell line (LNCaP) expressing full-length PTHrP or NLS-defective PTHrP. Overexpression of PTHrP in LNCaP cells significantly reduced *TNF* gene expression, while NLS-defective PTHrP failed to do so, supporting a negative correlation between *PTHLH* expression and *TNF* (Fig. 6A). Data from Figs 1, 2, 3, 4, 5, 6 and Table 1 all together demonstrated that prostate tumor cells expressing higher PTHrP have increased resistance to anoikis by suppressing a proapoptotic gene (*TNF*).

Recombinant TNF-α promotes anoikis and neutralizing TNF-α protects cells from anoikis

The causal role of TNF-α in PTHrP-dependent anoikis was further examined. Recombinant human TNF-α administration promoted anoikis in empty vector control PC-3 cells (Fig. 6B). More importantly, neutralizing TNF-α reduced the percentage of apoptotic PTHrP-knockdown PC-3 cells in an *in vitro* anoikis experiment model (Fig. 6C). These results establish the

Table 1

Gene	Detachment-induced genes (fold) (A) PTHrP-KD PC-3	(B) EV-control PC-3	(C) Fold changes ((A)/(B))
TNF	**4.829922**	**1.182631**	**4.08**
CD40LG	1.571345	0.547906	2.87
BAK1	1.285206	0.693515	1.85
TNFSF8	1.134455	0.688725	1.65
GADD45A	1.387031	0.865737	1.60
BIRC8	2.891865	1.830198	1.58
PYCARD	0.612168	1.126619	0.54
HRK	1.118837	2.993846	0.37
CIDEA	0.53663	1.45599	0.37
TP73	0.185823	0.890076	0.21

PC-3^{Luc} cells were transfected with *PTHLH*-targeting shRNA or empty lentiviral vectors, and stable clones were selected (designated PTHrP-KD and EV-control respectively). Cells were grown on a regular tissue-culture dish (control) and on agarose-covered plate to induce anoikis. Total RNA was prepared, followed by reverse transcription and quantitative PCR apoptotic gene array. Detachment-induced genes and fold induction in *PTHrP*-knockdown PC-3 cells are shown in column (A) (i.e. detachment effects in the *PTHrP*-knockdown clone = detached PTHrP-KD/attached PTHrP-KD), and those in empty vector control PC-3 cells (i.e. detachment effects in the control clone = detached EV-control/attached EV-control) are shown in column (B). To identify the anoikis genes altered by PTHrP reduction, fold changes comparing *PTHrP*-knockdown and control PC-3 cells are shown in column (C).

causal relationship between TNF-α and PTHrP-mediated anoikis in PC-3 cells.

Reduction of PTHrP expression decreased prostate cancer skeletal metastasis

The biological significance of PTHrP-dependent resistance to anoikis was examined using an experimental prostate cancer skeletal metastasis model. Prostate cancer cells expressing high PTHrP were anticipated to produce more metastatic lesions via increased survival in the bloodstream, compared to prostate cancer cells expressing low PTHrP (Fig. 7). In our previous experiments, PC-3 cells develop metastatic lesions predominantly in bones (i.e. hind limbs and mandibles) in an intracardiac injection model (Schneider *et al*. 2005, Park *et al*. 2011*a*). Accordingly, PTHrp-knockdown or empty vector PC-3^{Luc} cells were introduced into the systemic circulation and skeletal lesions were measured via *in vivo* bioluminescence imaging 5 weeks later. Because of differential *in vivo* growth rates (Fig. 1C), instead of comparing hind limb tumor size (quantified by photon emission from each lesion), incidence of hind limb metastatic lesions was reasoned to be a more appropriate comparison. *PTHrP*-knockdown PC-3^{Luc} (clone no. 10) produced significantly fewer hind limb metastatic lesions compared to empty vector control PC-3^{Luc} cells, potentially due to decreased survival from anoikis in the bloodstream.

Discussion

The current study demonstrated that tumor-derived PTHrP promotes prostate cancer metastasis, in part, by conferring resistance to anoikis, and that the PTHrP-dependent protection from anoikis is mediated by nuclear translocalization. Reduction of *PTHrP* gene expression in PC-3 ^{luc} human prostate cancer cells did not alter *in vitro* cellular proliferation but significantly decreased *in vivo* tumor growth, suggesting that PTHrP regulates cellular functions (evasion of apoptosis) in addition to previously known effects on proliferation. Indeed, PTHrP-knockdown cells had impaired ability to attach to the culture plates, leading to investigation of the mechanisms of PTHrP protection from anoikis. However, the discrepancy between *in vitro* proliferation and *in vivo* tumor growth might be attributable to other cellular functions. First, as wild-type PC-3 cells express high basal levels of PTHrP, reduction of PTHrP-expression to 20–40% (in PRHrp-knockdown clones 5 and 10) may not be sufficient to affect cellular proliferation, but enough to sensitize the cells to apoptotic stimuli. In addition, as PTHrP has been shown to regulate tumor angiogenesis (Liao *et al*. 2008), effects on *in vivo* tumor growth could simply be secondary to reduced angiogenesis. Murine endothelial cell-specific CD31/PECAM immunohistochemistry of the tumor tissue confirmed that PTHrP-knockdown tumors had significantly reduced mean vessel density (data not shown). Lastly, because PTHrP functions as a mediator in the crosstalk between the primary tumor and the bone/bone marrow, where a conducive environment is present, prostate tumors expressing low PTHrP may grow slower because of reduced recruitment of bone marrow-derived cells with tumorigenic functions (Park *et al*. 2011*b*). On the other hand, subsequent data (Figs 2, 3, 4 and 5) clearly demonstrated that PTHrP nuclear translocalization protects prostate tumor cells from anoikis, partly contributing to suppression of *in vivo* tumor growth of PTHrP-knockdown cells.

Antiapoptotic effects of PTHrP were first demonstrated in chondrocytes (Henderson *et al*. 1995), mediated by upregulation of the antiapoptotic protein BCL-2 (Amling *et al*. 1997). Later, PTHrP was shown to protect LoVo colon tumor cells from apoptosis by upregulating the PI3K/AKT pathway (Shen *et al*.

2007*b*). Additionally, PTHrP protected prostate tumor cells (C4-2 and PC-3) from chemotherapy-induced apoptosis in an intracrine manner (Bhatia *et al*. 2009*a*), of which observations were expanded by our current study. Therefore, PTHrP-mediated protection from apoptosis can be generalized to multiple inducers of apoptosis (e.g. chemotherapy, detachment, etc.), which can account for the correlation between PTHrP expression and metastatic potential of tumor cells (Hiraki *et al*. 2002, Liao & McCauley 2006). Apoptosis induced by disrupted epithelial cell–matrix interactions was described by Frisch & Francis (1994), and termed 'anoikis.' Evasion of anoikis was reasoned, and later proved to be a critical function of metastatic tumor cells (Yawata *et al*. 1998, Sakamoto *et al*. 2010). Data from the present study expand the role of PTHrP in protecting prostate tumor cells from anoikis, leading to decreased skeletal metastasis in PTHrP-knockdown cells compared to control PC-3 cells.

Interestingly, the PCR-based gene array data demonstrated that PTHrP prevents anoikis by down-regulating the proapoptotic gene *TNF*, which was confirmed in an additional human prostate cancer cell line. However, the mechanism of transcriptional downregulation by nuclear translocalization of PTHrP is unclear and requires further investigation. One potential mechanism underlying PTHrP-regulated gene expression is interaction with RNA. Aarts *et al*. (1999) demonstrated that nuclear PTHrP interacts with mRNA, which may lead to degradation of transcripts. Recently, deletion of mid-region, nuclear localization, and C-terminus of PTHrP (i.e. protein domains other than N-terminus which are recognized by the cognate receptor) decreases expression of genes essential for skeletal development (*Runx1*, *Runx2* and *Sox9*) while increasing expression of cell cycle inhibitors (p21 and p16), supporting a role for PTHrP in transcriptional regulation (Toribio *et al*. 2010). Therefore, despite lack of definitive experimental evidence, nuclear localization of PTHrP may play critical roles in regulating gene expression, resulting in cellular phenotypes such as protection from apoptosis.

The current study has potential clinical significance by providing an additional molecular mechanism contributing to prostate cancer skeletal metastasis. Reduction of PTHrP resulted in decreased metastatic

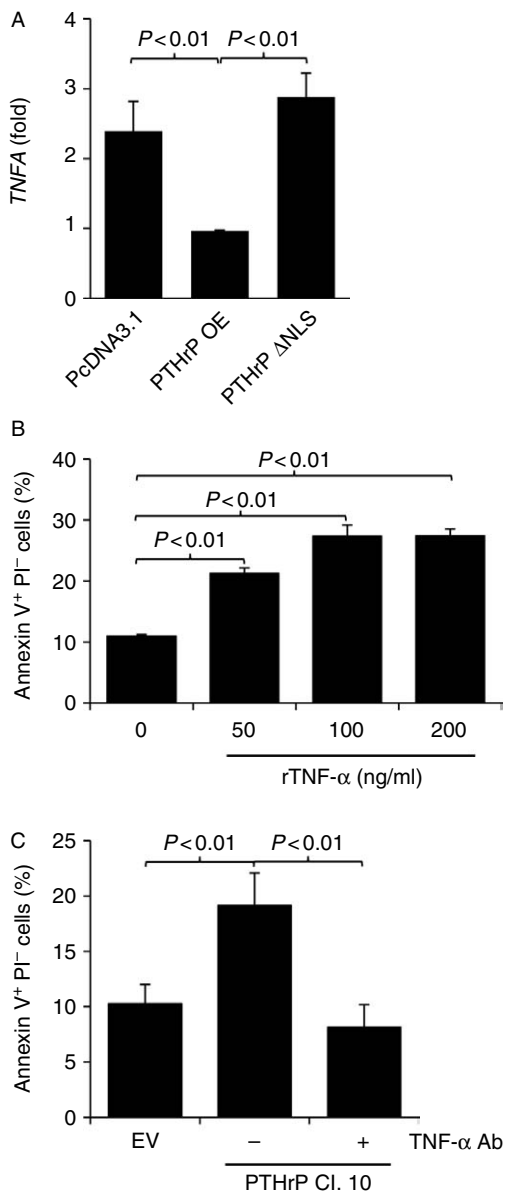

Figure 6 NLS-defective PTHrP failed to decrease *TNF* in response to detachment. (A) LNCaP cells were transfected with empty pcDNA3.1, PTHrP OE, or PTHrP ΔNLS vectors, and stable clones were selected. Cells were grown on regular tissue-culture dishes (control) and on agarose-covered plates to induce anoikis ($n=3$ each). Total RNA was prepared, followed by quantitative RT-PCR for *TNF* and *GAPDH* (for normalization). Normalized *TNF* gene expression from detached cells divided by normalized *TNF* expression from attached cells is shown graphically. Data are mean±S.D. $P<0.05$ by Student's *t*-test was considered statistically significant. (B) PC-3 empty vector control cells were seeded on agarose-covered plates to induce anoikis ($n=5$ each), followed by treatment with human recombinant TNF-α (0–200 ng/ml, as indicated). Apoptotic cells were quantified by flow cytometric analyses of Annexin V^+PI^- cells. Data are mean± S.D. $P<0.05$ by Student's *t*-test was considered statistically significant. (C) PTHrP-knockdown (clone no. 10) or empty vector control PC-3 cells were seeded on agarose-covered six-well plates to induce anoikis ($n=5$ each).
Anti-human TNF-α antibody (0.6 μg/ml) was added to neutralize TNF-α in the culture supernatant. Apoptotic cells were quantified by flow cytometric analyses of Annexin V^+PI^- cells. Data are mean±S.D. $P<0.05$ by Student's *t*-test was considered statistically significant.

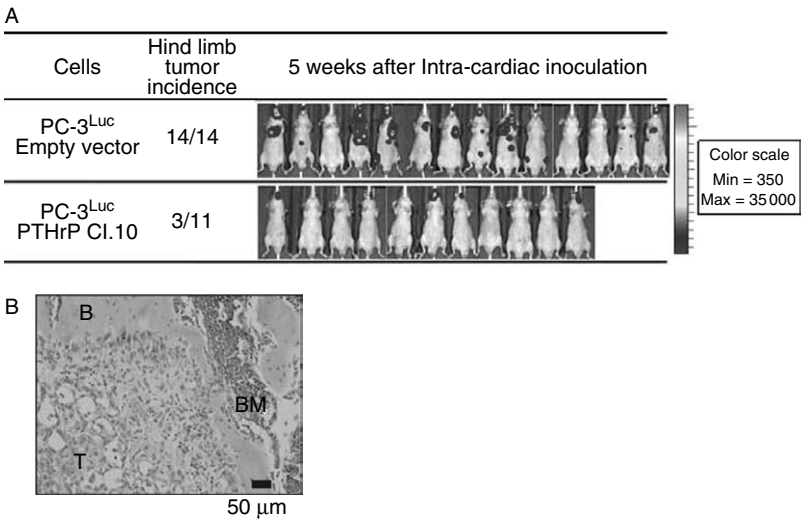

Figure 7 Reduction of PTHrP expression decreased prostate cancer skeletal metastasis. (A) PTHrP-knockdown (clone no. 10) or empty vector control PC-3^{Luc} cells were inoculated into the systemic circulation to compare skeletal metastasis in male athymic mice ($n=14$ for empty vector transfected group and $n=11$ for PTHrP-knockdown clone 10 group). Development of metastatic lesions was determined by bioluminescence imaging. Hind limbs emitting more than 1×10^5 photons/s were considered metastases, and mice carrying one or more metastatic hind limbs were counted and presented. There was a statistically significant difference ($P<0.01$ by Fisher's exact test) in the incidence of hind limb metastatic lesions between the two groups. The whole body bioluminescence images of all mice in the experiment are shown. Note that not all metastatic lesions appear in colors, because of the normalization of pseudocoloring to the highest bioluminescence signals (mostly mandibular lesions in the control group). (B) A representative microscopic image of a metastatic lesion in the proximal tibia of PC-3^{Luc} empty vector cells. T, tumor cells; B, bone; BM, bone marrow.

lesions in an experimental skeletal metastasis model. Incidence of skeletal metastatic lesions in hind limbs was significantly lower than the empty vector control group, not to mention hind limb metastatic tumor size (as determined by average photon emission from metastatic lesions in each group). However, we reasoned that the comparison of tumor size between two groups may not be an adequate approach to analyze the data, because two clones (empty vector control clone and PTHrP-knockdown clone) had significantly different growth potential *in vivo*, thus the hind limb tumor size quantification was not included in the data. Instead, as PTHrP-knockdown cells produced significantly fewer metastatic lesions in the hind limbs compared to 100% development of hind limb metastasis in the empty vector control cells, this likely reflects the altered ability for cells to survive the trajectory from injection to tumor cell lodging and growth in bone.

In conclusion, the current study demonstrates a role for PTHrP in protecting prostate tumor cells from anoikis *in vitro*, downregulating *TNF* gene expression, and supporting metastatic potential of prostate tumor cells *in vivo*.

Declaration of interest

The authors declare that there is no conflict of interest that could be perceived as prejudicing the impartiality of the research reported.

Funding

This work was financially supported by the US Department of Defense Prostate Cancer Research Program Grants (grant numbers W81XWH-10-1-0546 (S I Park) and W81XWH-08-1-0037 (L K McCauley)); and the US National Cancer Institute Program Project Grant (grant number P01CA093900 (L K McCauley)).

Author contribution statement

L K McCauley supervised all experiments and manuscript preparation. S I Park and L K McCauley designed the experiments and analyzed the data. S I Park performed the experiments and wrote the manuscript.

Acknowledgements

The authors thank Janice E Berry, Amy J Koh, and Matthew Eber for their assistance in the preparation of this manuscript, and Thomas J Rosol for providing the Ace-1 prostate cancer cells.

References

Aarts MM, Levy D, He B, Stregger S, Chen T, Richard S & Henderson JE 1999 Parathyroid hormone-related protein interacts with RNA. *Journal of Biological Chemistry* **274** 4832–4838. (doi:10.1074/jbc.274.8.4832)

Amling M, Neff L, Tanaka S, Inoue D, Kuida K, Weir E, Philbrick WM, Broadus AE & Baron R 1997 Bcl-2 lies downstream of parathyroid hormone-related peptide in a signaling pathway that regulates chondrocyte maturation during skeletal development. *Journal of Cell Biology* **136** 205–213. (doi:10.1083/jcb.136.1.205)

Bhatia V, Mula RV, Weigel NL & Falzon M 2009*a* Parathyroid hormone-related protein regulates cell survival pathways via integrin alpha6beta4-mediated activation of phosphatidylinositol 3-kinase/Akt signaling. *Molecular Cancer Research* **7** 1119–1131. (doi:10.1158/1541-7786.MCR-08-0568)

Bhatia V, Saini MK & Falzon M 2009*b* Nuclear PTHrP targeting regulates PTHrP secretion and enhances LoVo cell growth and survival. *Regulatory Peptides* **158** 149–155. (doi:10.1016/j.regpep.2009.07.008)

Deftos LJ, Barken I, Burton DW, Hoffman RM & Geller J 2005 Direct evidence that PTHrP expression promotes prostate cancer progression in bone. *Biochemical and Biophysical Research Communications* **327** 468–472. (doi:10.1016/j.bbrc.2004.11.162)

Dougherty KM, Blomme EA, Koh AJ, Henderson JE, Pienta KJ, Rosol TJ & McCauley LK 1999 Parathyroid hormone-related protein as a growth regulator of prostate carcinoma. *Cancer Research* **59** 6015–6022.

Downey SE, Hoyland J, Freemont AJ, Knox F, Walls J & Bundred NJ 1997 Expression of the receptor for parathyroid hormone-related protein in normal and malignant breast tissue. *Journal of Pathology* **183** 212–217. (doi:10.1002/(SICI)1096-9896(199710)183:2<212::AID-PATH920>3.0.CO;2-O)

Frisch SM & Francis H 1994 Disruption of epithelial cell–matrix interactions induces apoptosis. *Journal of Cell Biology* **124** 619–626. (doi:10.1083/jcb.124.4.619)

Henderson JE, Amizuka N, Warshawsky H, Biasotto D, Lanske BM, Goltzman D & Karaplis AC 1995 Nucleolar localization of parathyroid hormone-related peptide enhances survival of chondrocytes under conditions that promote apoptotic cell death. *Molecular and Cellular Biology* **15** 4064–4075.

Hiraki A, Ueoka H, Bessho A, Segawa Y, Takigawa N, Kiura K, Eguchi K, Yoneda T, Tanimoto M & Harada M 2002 Parathyroid hormone-related protein measured at the time of first visit is an indicator of bone metastases and survival in lung carcinoma patients with hypercalcemia. *Cancer* **95** 1706–1713. (doi:10.1002/cncr.10828)

Iddon J, Bundred NJ, Hoyland J, Downey SE, Baird P, Salter D, McMahon R & Freemont AJ 2000 Expression of parathyroid hormone-related protein and its receptor in bone metastases from prostate cancer. *Journal of Pathology* **191** 170–174. (doi:10.1002/(SICI)1096-9896(200006)191:2<170::AID-PATH620>3.0.CO;2-H)

Iwamura M, di Sant'Agnese PA, Wu G, Benning CM, Cockett AT, Deftos LJ & Abrahamsson PA 1993 Immunohistochemical localization of parathyroid hormone-related protein in human prostate cancer. *Cancer Research* **53** 1724–1726.

Jemal A, Bray F, Center MM, Ferlay J, Ward E & Forman D 2011 Global cancer statistics. *CA: A Cancer Journal for Clinicians* **61** 69–90. (doi:10.3322/caac.20107)

Langley RR & Fidler IJ 2011 The seed and soil hypothesis revisited – the role of tumor–stroma interactions in metastasis to different organs. *International Journal of Cancer* **128** 2527–2535. (doi:10.1002/ijc.26031)

LeRoy BE, Thudi NK, Nadella MV, Toribio RE, Tannehill-Gregg SH, van Bokhoven A, Davis D, Corn S & Rosol TJ 2006 New bone formation and osteolysis by a metastatic, highly invasive canine prostate carcinoma xenograft. *Prostate* **66** 1213–1222. (doi:10.1002/pros.20408)

Li X, Koh AJ, Wang Z, Soki FN, Park SI, Pienta KJ & McCauley LK 2011 Inhibitory effects of megakaryocytic cells in prostate cancer skeletal metastasis. *Journal of Bone and Mineral Research* **26** 125–134. (doi:10.1002/jbmr.204)

Liao J & McCauley LK 2006 Skeletal metastasis: established and emerging roles of parathyroid hormone related protein (PTHrP). *Cancer Metastasis Reviews* **25** 559–571.

Liao J, Li X, Koh AJ, Berry JE, Thudi N, Rosol TJ, Pienta KJ & McCauley LK 2008 Tumor expressed PTHrP facilitates prostate cancer-induced osteoblastic lesions. *International Journal of Cancer* **123** 2267–2278. (doi:10.1002/ijc.23602)

Minard ME, Ellis LM & Gallick GE 2006 Tiam1 regulates cell adhesion, migration and apoptosis in colon tumor cells. *Clinical & Experimental Metastasis* **23** 301–313. (doi:10.1007/s10585-006-9040-z)

Moseley JM, Kubota M, Diefenbach-Jagger H, Wettenhall RE, Kemp BE, Suva LJ, Rodda CP, Ebeling PR, Hudson PJ, Zajac JD *et al.* 1987 Parathyroid hormone-related protein purified from a human lung cancer cell line. *PNAS* **84** 5048–5052. (doi:10.1073/pnas.84.14.5048)

Park SI, Kim SJ, McCauley LK & Gallick GE 2011*a* Pre-clinical mouse models of human prostate cancer and their utility in drug discovery. *Current Protocols in Pharmacology* **51** Chapter 14:Unit 14.15.

Park SI, Soki FN & McCauley LK 2011*b* Roles of bone marrow cells in skeletal metastases: no longer bystanders. *Cancer Microenvironment* **4** 237–246. (doi:10.1007/s12307-011-0081-8)

Ratcliffe WA, Norbury S, Heath DA & Ratcliffe JG 1991 Development and validation of an immunoradiometric assay of parathyrin-related protein in unextracted plasma. *Clinical Chemistry* **37** 678–685.

Sakamoto S & Kyprianou N 2010 Targeting anoikis resistance in prostate cancer metastasis. *Molecular Aspects of Medicine* **31** 205–214. (doi:10.1016/j.mam.2010.02.001)

Sakamoto S, McCann RO, Dhir R & Kyprianou N 2010 Talin1 promotes tumor invasion and metastasis via focal adhesion signaling and anoikis resistance. *Cancer Research* **70** 1885–1895. (doi:10.1158/0008-5472.CAN-09-2833)

Schneider A, Kalikin LM, Mattos AC, Keller ET, Allen MJ, Pienta KJ & McCauley LK 2005 Bone turnover mediates preferential localization of prostate cancer in the skeleton. *Endocrinology* **146** 1727–1736. (doi:10.1210/en.2004-1211)

Shen X, Mula RV, Evers BM & Falzon M 2007*a* Increased cell survival, migration, invasion, and Akt expression in PTHrP-overexpressing LoVo colon cancer cell lines. *Regulatory Peptides* **141** 61–72. (doi:10.1016/j.regpep.2006.12.017)

Shen X, Rychahou PG, Evers BM & Falzon M 2007*b* PTHrP increases xenograft growth and promotes integrin alpha6beta4 expression and Akt activation in colon cancer. *Cancer Letters* **258** 241–252. (doi:10.1016/j.canlet.2007.09.010)

Suva LJ, Winslow GA, Wettenhall RE, Hammonds RG, Moseley JM, Diefenbach-Jagger H, Rodda CP, Kemp BE, Rodriguez H, Chen EY *et al.* 1987 A parathyroid hormone-related protein implicated in malignant hypercalcemia: cloning and expression. *Science* **237** 893–896. (doi:10.1126/science.3616618)

Thudi NK, Martin CK, Murahari S, Shu ST, Lanigan LG, Werbeck JL, Keller ET, McCauley LK, Pinzone JJ & Rosol TJ 2011 Dickkopf-1 (DKK-1) stimulated prostate cancer growth and metastasis and inhibited bone formation in osteoblastic bone metastases. *Prostate* **71** 615–625. (doi:10.1002/pros.21277)

Toribio RE, Brown HA, Novince CM, Marlow B, Hernon K, Lanigan LG, Hildreth BE III, Werbeck JL, Shu ST, Lorch G *et al.* 2010 The midregion, nuclear localization sequence, and C terminus of PTHrP regulate skeletal development, hematopoiesis, and survival in mice. *FASEB Journal* **24** 1947–1957. (doi:10.1096/fj.09-147033)

Weilbaecher KN, Guise TA & McCauley LK 2011 Cancer to bone: a fatal attraction. *Nature Reviews. Cancer* **11** 411–425. (doi:10.1038/nrc3055)

Yawata A, Adachi M, Okuda H, Naishiro Y, Takamura T, Hareyama M, Takayama S, Reed JC & Imai K 1998 Prolonged cell survival enhances peritoneal dissemination of gastric cancer cells. *Oncogene* **16** 2681–2686. (doi:10.1038/sj.onc.1201792)

Received in final form 24 January 2012
Accepted 30 January 2012
Made available online as an Accepted Preprint
30 January 2012

Microenvironment and Immunology

Cancer Research

Cyclophosphamide Creates a Receptive Microenvironment for Prostate Cancer Skeletal Metastasis

AU Serk In Park[1], Jinhui Liao[1], Janice E. Berry[1], Xin Li[1], Amy J. Koh[1], Megan E. Michalski[1], Matthew R. Eber[1], Fabiana N. Soki[1], David Sadler[1], Sudha Sud[2], Sandra Tisdelle[5], Stephanie D. Daignault[4], Jeffrey A. Nemeth[6], Linda A. Snyder[6], Thomas J. Wronski[5], Kenneth J. Pienta[2], and Laurie K. McCauley[1,3]

Abstract

A number of cancers predominantly metastasize to bone, due to its complex microenvironment and multiple types of constitutive cells. Prostate cancer especially has been shown to localize preferentially to bones with higher marrow cellularity. Using an experimental prostate cancer metastasis model, we investigated the effects of cyclophosphamide, a bone marrow–suppressive chemotherapeutic drug, on the development and growth of metastatic tumors in bone. Priming the murine host with cyclophosphamide before intracardiac tumor cell inoculation was found to significantly promote tumor localization and subsequent growth in bone. Shortly after cyclophosphamide treatment, there was an abrupt expansion of myeloid lineage cells in the bone marrow and the peripheral blood, associated with increases in cytokines with myelogenic potential such as C-C chemokine ligand (CCL)2, interleukin (IL)-6, and VEGF-A. More importantly, neutralizing host-derived murine CCL2, but not IL-6, in the premetastatic murine host significantly reduced the prometastatic effects of cyclophosphamide. Together, our findings suggest that bone marrow perturbation by cytotoxic chemotherapy can contribute to bone metastasis via a transient increase in bone marrow myeloid cells and myelogenic cytokines. These changes can be reversed by inhibition of CCL2. *Cancer Res; 72(00); 1–11. ©2012 AACR.*

Introduction

Bone is the predominant site of prostate cancer metastasis, and patients with advanced-stage prostate cancer commonly develop metastatic bone lesions (1). Unfortunately, the pathophysiology of skeletal metastasis is not yet completely understood (2). One major obstacle to better understanding skeletal metastasis is the unusual complexity of the tumor microenvironment in bone (3), due to multiple constituent cell types. Emerging evidence supports that cells in the bone marrow microenvironment are actively involved in prostate cancer metastasis (4).

Bone marrow–derived myeloid lineage cells are critical regulators of tumor progression and metastasis (5–10). Yang and colleagues showed that expansion of Gr-1$^+$CD11b$^+$ myeloid cells directly promotes tumor angiogenesis (6) via increased production of matrix metalloproteinase (MMP)-9 (7). Myeloid cells (expressing surface markers CD11b and/or Gr-1) are a major component of undifferentiated bone marrow cells, and ultimately differentiate into monocytes, macrophages, and granulocytes (10). Parallel to the tumorigenic roles of myeloid cells, monocyte macrophages also have been shown to participate in tumor metastasis (11–13). All of these data collectively support the critical roles of myeloid lineage cells in prostate cancer progression and bone metastasis. However, it is not clearly understood how the alterations in the bone marrow occur, which could provide clues for therapeutic approaches.

In clinical settings, chemotherapeutic drugs and/or irradiation perturb the bone marrow microenvironment, leading to alterations in marrow cellular composition. Although chemotherapy and irradiation are both bone marrow suppressive, the subsequent recovery process may lead to temporary spikes of certain cell types, including monocytes and neutrophils (14, 15). Therefore, net effects of bone marrow–suppressive agents could have pro- or antitumorigenic effects. Interestingly, priming the murine host with cyclophosphamide, a bone marrow–suppressive chemotherapeutic drug, promoted subcutaneous tumor growth and metastasis in several mouse models (16–19). Cyclophosphamide is a DNA-alkylating drug commonly included in chemotherapeutic regimens against breast and lung cancers and non-Hodgkin's lymphoma. In addition, cyclophosphamide is used in the conditioning regimen for recipients of myeloablative bone marrow transplantation, to enhance engraftment and suppress the host immune reaction. Intriguing data showing opposite prometastatic effects of chemotherapeutic drugs remain poorly investigated.

Authors' Affiliations: Departments of [1]Periodontics and Oral Medicine, [2]Internal Medicine, and [3]Pathology, [4]Cancer Center Biostatistics Core, University of Michigan, Ann Arbor, Michigan; [5]Department of Physiological Sciences, University of Florida, Gainesville, Florida; and [6]Janssen Research and Development, LLC, Radnor, Pennsylvania

Note: Supplementary data for this article are available at Cancer Research Online (http://cancerres.aacrjournals.org/).

Corresponding Author: Laurie K. McCauley, University of Michigan School of Dentistry, Room 3343, 1011 N. University Ave., Ann Arbor, MI 48109. Phone: 1-734-647-3206; Fax: 1-734-763-5503; E-mail: mccauley@umich.edu

doi: 10.1158/0008-5472.CAN-11-2928

To our best knowledge, the effects of cyclophosphamide on skeletal metastasis have never been reported. Given that prostate cancer has been shown to use similar strategies as hematopoietic stem/progenitor cell homing and that prostate cancer has long been known to home typically to bones enriched with red marrow (20), we hypothesized that alterations induced by cyclophosphamide in the bone marrow microenvironment would contribute to prostate cancer colonization in the bone and/or subsequent tumor growth. In the current study, we investigated prometastatic effects of bone marrow suppression in a prostate cancer skeletal metastasis model and explored the underlying mechanisms that could be used to design methods of therapeutic intervention.

Materials and Methods

Cells

Luciferase-labeled PC-3 cells (PC-3^{Luc}) were established from the PC-3 cell line (American Type Culture Collection; ATCC), as previously described (20). PC-3^{Luc} cells were regularly authenticated and matched short tandem repeat DNA profiles of the original PC-3 cell line (last tested on May 9, 2009).

Mouse models of prostate cancer

All experimental protocols were approved by the University of Michigan Institutional Animal Care and Use Committee. For a skeletal metastasis model, the procedure described by Park and colleagues was followed (21). Briefly, 2×10^5 PC-3^{Luc} cells were injected into the left heart ventricle of male athymic mice (Harlan Laboratories). For an orthotopic bone tumor model, 1×10^3 PC-3^{Luc} cells were injected in the proximal tibiae as described (21).

Ex vivo murine bone marrow microvascular angiography

Murine bone marrow vasculature was visualized by a modified method of Guldberg and colleagues (22) Mice were anesthetized and perfused sequentially with heparin-supplemented Ringer's lactate (9 minutes), formalin (9 minutes), and MICROFIL (Flow Tech, 7 minutes) via the intracardiac route. Following polymerization, femurs were dissected, decalcified, and scanned by microcomputed tomography (μCT).

Neutralizing antibodies

Anti-mouse CCL2 antibody (C1142, Janssen) and anti-mouse interleukin (IL)-6 antibody (R&D Systems) were provided by Janssen, LLC. C1142 is a rat/mouse chimeric antibody specific for mouse C-C chemokine ligand (CCL)2/MCP-1 and does not cross-react with human CCL2 or mouse MCP-5 (23–25). Nonspecific IgG from mouse serum (Sigma-Aldrich) was used as a control antibody.

Flow cytometry

Bone marrow cells were collected by flushing femurs and tibiae. Lungs, liver, and kidney were digested in complete Dulbecco's Modified Eagle's Medium supplemented with 0.5 mg/mL collagenase (Sigma-Aldrich). One million cells were used for flow cytometry (BD Bioscience).

Complete blood counting with white blood cell differentials

Blood cell counting was carried out in the University of Michigan Unit for Laboratory Animal Medicine, using a Forcyte automatic hematology analyzer (Oxford Science).

Quantitative PCR

The mRNA samples were prepared from the flushed bone marrow cells, followed by ~~RT-PCR~~ for *CD31* and mouse glyceraldehyde-3-phosphate dehydrogenase (*GAPDH*; Applied Biosystems).

Statistical analyses

Experimental skeletal metastasis experiments were analyzed using linear mixed models. The primary outcome was the natural log transformed bioluminescence measurement. Fixed covariates in the model included the groups in the experiment and time (weeks) and the interaction between group and time. The repeated measures aspect of the model, due to multiple measurements over time within each mouse, was adjusted for using a single order autoregressive correlation structure. Contrasts were used to test the pairwise comparisons of interest. Analyses were completed using SAS (SAS Institute) with a type I error of 5%.

All other statistical analyses, including Kaplan–Meier analyses of metastasis-free mice, Student t tests comparing 2 groups, and Mann–Whitney U tests of samples failing to distribute normally, were conducted with GraphPad Prism.

Results

Cyclophosphamide enhanced experimental prostate cancer skeletal metastasis *in vivo*

Cyclophosphamide has been shown to promote subcutaneous tumor growth and experimental metastasis in various animal models (16–19). Initially, the effects of cyclophosphamide on prostate cancer skeletal metastasis were investigated. The experimental design is schematically shown in Fig. 1A. The serum half-life of cyclophosphamide is less than 17 minutes (in mice) and 6.5 hours (in human), and mice were allowed 7 days of recovery to insure that the drug was completely cleared, to avoid any direct antitumor effects of cyclophosphamide (26, 27). Interestingly, mice primed with cyclophosphamide developed significantly larger tumors in the hind limb bones after 7 days (Fig. 1B). Cyclophosphamide-treated mice exhibited increased tumor bioluminescence in the mandible also, but the effects were variable and not statistically significant until day 35 (Fig. 1C). Because hind limb skeletal metastases are more clinically relevant, and also murine mandibles are significantly different from human (e.g., continuous eruption of incisors), the hind limb skeletal metastases were the focus of subsequent investigation. Cyclophosphamide-primed mice developed hind limb metastases at an earlier time point (i.e., increased incidence of metastases on day 7, 14, and 21; Fig. 1D), compared with the saline-treated group that developed detectable hind limb metastatic lesions only after 14 days. These data suggest that the larger tumor size on day 42 in the hind limbs of cyclophosphamide-treated mice (Fig. 1E) is

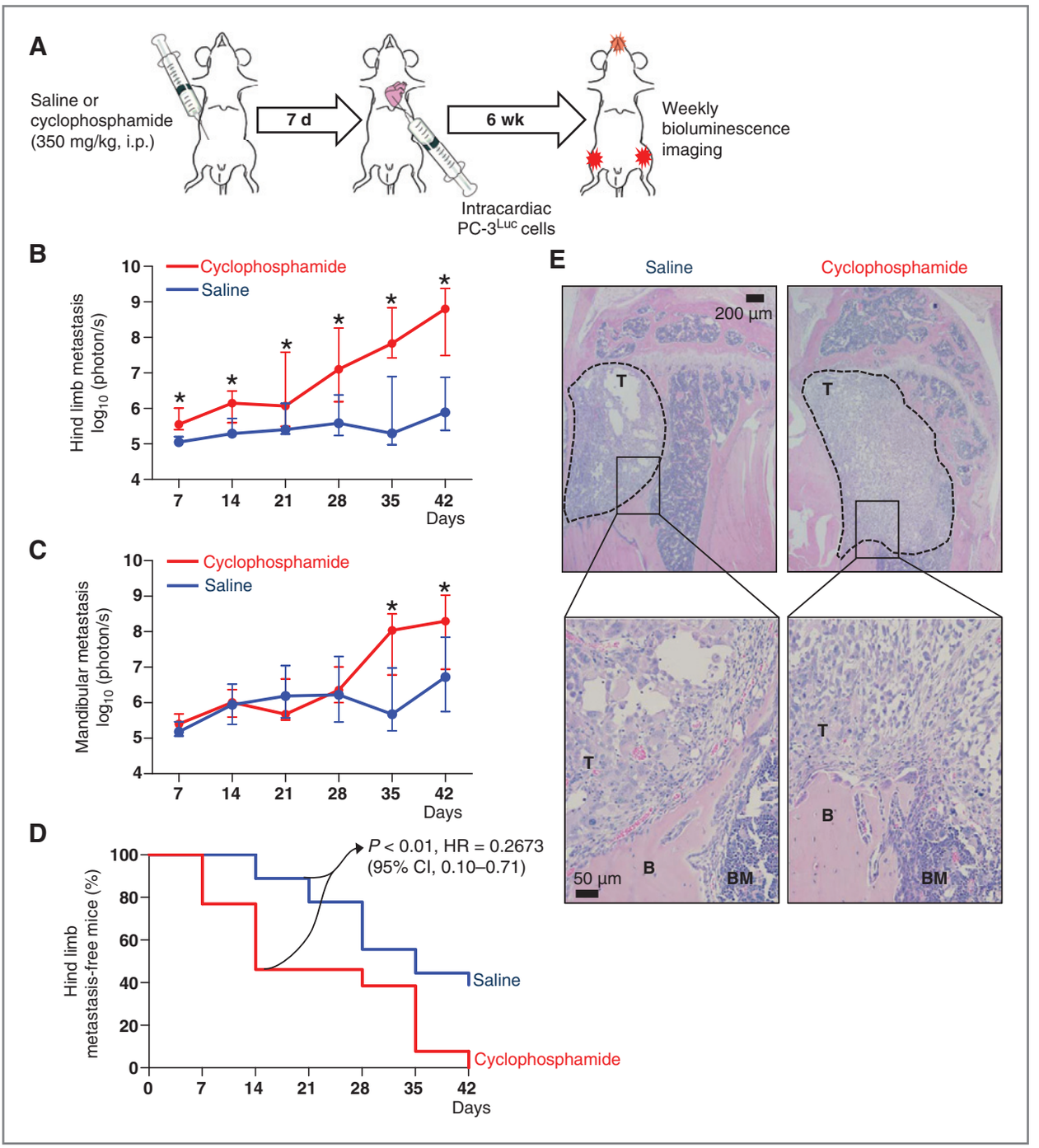

Figure 1. Priming mice with a single administration of cyclophosphamide (CY) enhanced experimental prostate cancer skeletal metastasis. A, schematic representation of the experimental design. Male athymic mice were divided into 2 groups and treated with saline or CY. Following 7 days of recovery, PC-3^{Luc} cells were injected into the left heart ventricle ($n = 18$ for saline control and $n = 13$ for CY group). Metastatic tumor growth was monitored by weekly *in vivo* bioluminescence imaging for 6 weeks. B, hind limb metastatic tumor size was measured by weekly *in vivo* bioluminescence imaging. Data are medians with interquartile range. Asterisks represent statistical significance (linear contrasts $P < 0.01$). C, mandibular metastatic tumor size was measured. Data are median $\pm$ interquartile range. Asterisks represent statistical significance (linear contrasts $P < 0.01$). D, percentage of hind limb metastasis-free mice plotted in a Kaplan–Meier curve. Lesions emitting more than 1×10^5 photon/sec were considered as metastases, and statistical significance was determined by log-rank test ($P < 0.01$). E, representative histologic images of metastatic bone tumors. Tumor-bearing hind limb tibiae were dissected, followed by hematoxylin and eosin (H&E) staining. The presence of metastatic tumor cells was confirmed microscopically. Tumor perimeter is indicated by dotted lines in lower magnification images ($\times$ 4; top). Higher magnification images ($\times$ 20; bottom) show tumor, bone, and bone marrow (denoted T, B, and BM, respectively). Q4

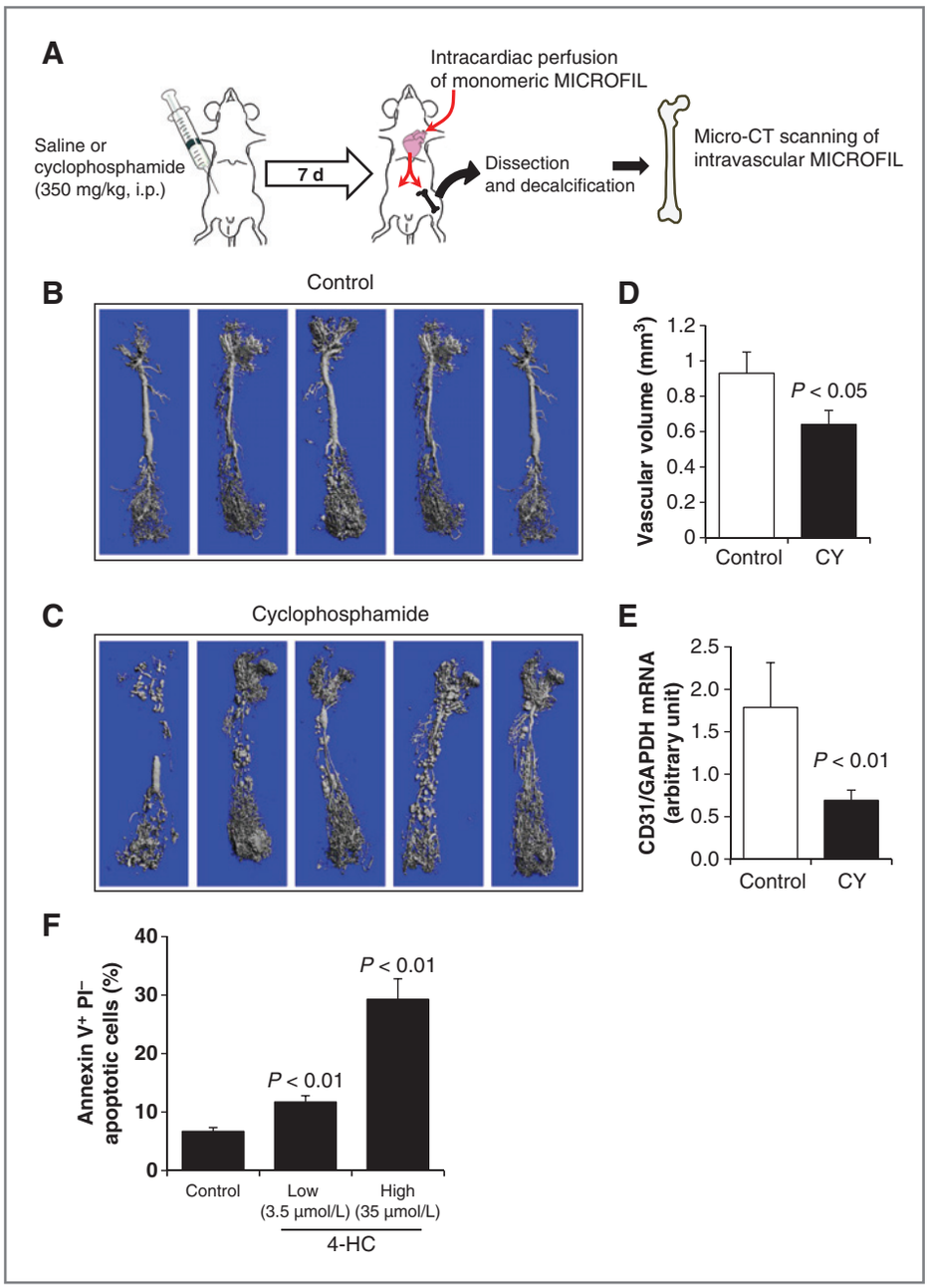

Figure 2. A single administration of cyclophosphamide (CY) significantly disrupted bone marrow vascular integrity. A, schematic representation of *ex vivo* murine bone marrow microvascular angiography. Male C57BL6/J mice were divided into 2 groups ($n = 13$/group) and treated with saline or CY. Following 7 days of recovery, mice were perfused with liquid-phase radiopaque monomeric compound via the intracardiac route. After polymerization, femurs were dissected, decalcified, and scanned with µCT. B, five representative µCT images of *ex vivo* femoral angiography from the saline-treated group ($n = 13$) are shown. C, five representative µCT images of *ex vivo* femoral angiography from the CY-treated group ($n = 13$) are shown. D, µCT data were analyzed to quantify the total vascular volume (per bone). Data are mean ± SEM ($P < 0.05$ by Mann–Whitney *U* test). E, femurs of saline- or CY-treated C57B6/J mice ($n = 10$/group; the same dosage and schedule as described in A–C) were dissected, and bone marrow was harvested. The mRNA expression of *CD31/PECAM* endothelial cell marker was determined by quantitative RT-PCR. Data are mean ± SD ($P < 0.01$ by the Student *t* test). F, human bone marrow endothelial cells were cultured and treated with low (3.5 µmol/L) and high (35 µmol/L) concentrations of 4-HC, metabolite of CY with *in vitro* activity, for 24 hours. The percentage of apoptotic cells was determined by flow cytometry [Annexin V^+ and propidium iodide (PI^-)]. Data are mean ± SEM ($n = 6$/group; $P < 0.01$ by the Student *t* test).

attributable to the early events following tumor cell inoculation.

A single dose of cyclophosphamide significantly disrupted bone marrow vascular integrity

Cyclophosphamide has been found to cause damage to endothelial cells, potentially promoting tumor cell seeding in the metastatic target organs (28). These data are consistent with the observation in Fig. 1 showing outgrowth of metastatic tumors at earlier time points in the cyclophosphamide-treated hosts. Consequently, an experiment was designed to test whether a single dose of cyclophosphamide could perturb endothelial integrity in the bone marrow, which might in turn lead to increased extravasation of tumor cells immediately after inoculation. Because immunohistochemistry can only provide 2-dimensional images of selected cross-sections, a technique to reconstruct 3-dimensional vascular structures enclosed in calcified tissues was used (ref. 22; Fig. 2A). In Fig. 2B, this technique clearly showed 3-dimensional structures of microvessels in the epiphyses and the central sinusoidal vessels in the diaphyses of saline controls. In sharp contrast, a single dose of cyclophosphamide very obviously disrupted vascular integrity and continuity (Fig. 2C). Quantification of the images in Fig. 2B and C showed that bone marrow vascular volume was

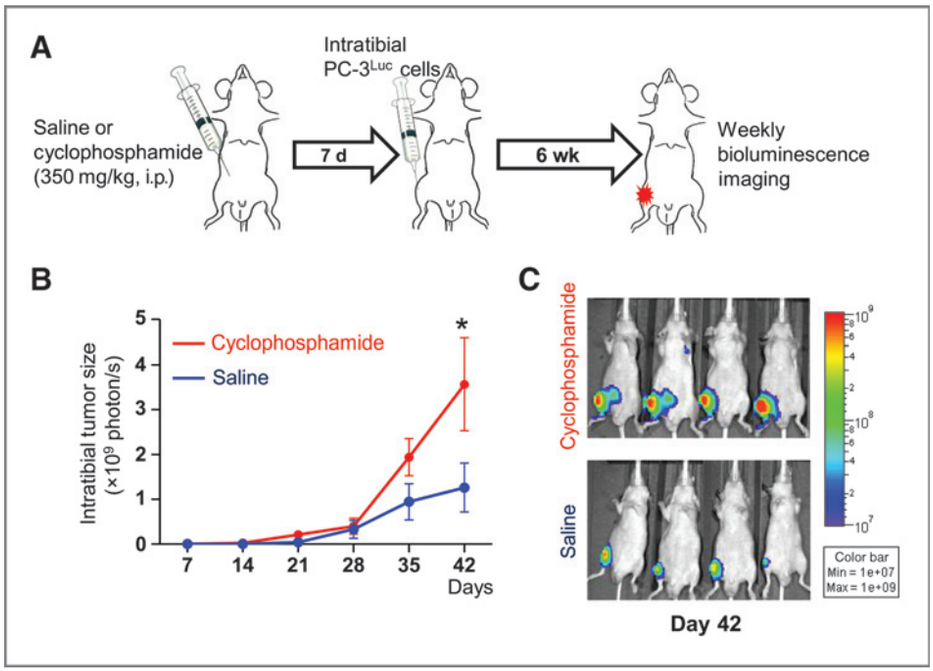

Figure 3. Cyclophosphamide (CY) pretreatment directly promoted orthotopic PC-3 tumor growth in bone. A, schematic representation of the experiment. Male athymic mice were divided into 2 groups ($n = 8$/group) and treated with saline or CY. Following 7 days of recovery, PC-3^{Luc} cells were injected into the bone marrow space of the right proximal tibiae. Tumor growth in bone was monitored by weekly *in vivo* bioluminescence imaging for 6 weeks. B, intratibial tumor size was measured by weekly *in vivo* bioluminescence imaging ($P < 0.05$ by the Student *t* test). Data are mean ± SEM. C, representative images of *in vivo* bioluminescence on day 42.

significantly reduced by cyclophosphamide (Fig. 2D). *CD31* (an endothelial-specific marker) gene expression in bone was significantly suppressed with cyclophosphamide administration (Fig. 2E), but not in lungs, liver, and kidney (Supplementary Fig. S1). In addition, bone marrow endothelial cells treated with 4-hydroperoxycyclophosphamide (4-HC, a metabolite of cyclophosphamide with *in vitro* biologic activity) had significantly increased apoptosis (Fig. 2F). Taken together, cyclophosphamide-induced vascular disruption led to altered endothelial cells in the bone marrow.

Cyclophosphamide treatment did not cause systemic inflammation

We next ruled out the possibility that cyclophosphamide promoted metastasis by systemic inflammation secondary to the bone marrow suppression. Cyclophosphamide-treated mice had significantly reduced body weight, compared with the saline control groups, and the effects lasted more than 2 weeks (Supplementary Fig. S2A). However, cyclophosphamide-treated mice regained body weight with a similar trend to the saline-treated controls. In addition, cyclophosphamide-treated mice did not show any significant lethargy or signs of systemic inflammation, the latter often signaled by increased circulating levels of C-reactive protein (Supplementary Fig. S2B).

Cyclophosphamide pretreatment promoted orthotopic prostate tumor growth in bone

The potential role of disrupted bone marrow vascular integrity secondary to cyclophosphamide treatment in the increased metastatic tumor growth in the bone was further tested using an orthotopic approach (Fig. 3A). This approach was designed to circumvent the effects of vascular disruption that could contribute to initial tumor cell seeding. PC-3 tumors grew larger after 6 weeks in the cyclophosphamide-treated bone marrow, than in control (Fig. 3B and C), suggesting that alterations in the cyclophosphamide-treated murine bone marrow, not a specific compromise of vascular integrity, were responsible for promoting tumor growth and/or metastasis.

Cyclophosphamide transiently expanded myeloid lineage cells

On the basis of the observation in Figs. 2 and 3, alterations induced by cyclophosphamide potentially contributing to tumor growth and/or metastasis were investigated. The changes of white blood cell (WBC) differential counts were further investigated serially after cyclophosphamide administration. Total WBC counts were significantly reduced 3 to 15 days after cyclophosphamide, indicating that cyclophosphamide suppressed bone marrow, and that the effects lasted more than 2 weeks (Fig. 4A). However, the WBC count was increased on day 7 compared with the day 3 cyclophosphamide group (Fig. 4A). Furthermore, neutrophil number was below detection on day 3 but significantly spiked on day 7, immediately followed by suppression (Fig. 4B). In addition, monocyte counts showed a similar pattern to neutrophils (Fig. 4C). Collectively, these data revealed that differentiated myeloid cells in the peripheral blood (i.e., monocytes and neutrophils) transiently increased during recovery from cyclophosphamide.

Because both monocytes and neutrophils are differentiated from myeloid lineage cells in the bone marrow, the nature of the changes of myeloid lineage cells in the bone marrow was determined. Flow cytometric analyses of bone marrow cells from mice treated with cyclophosphamide after 3, 7, 10, and 15 days revealed that myeloid lineage cells (expressing CD11b) were significantly expanded 7 and 10 days after

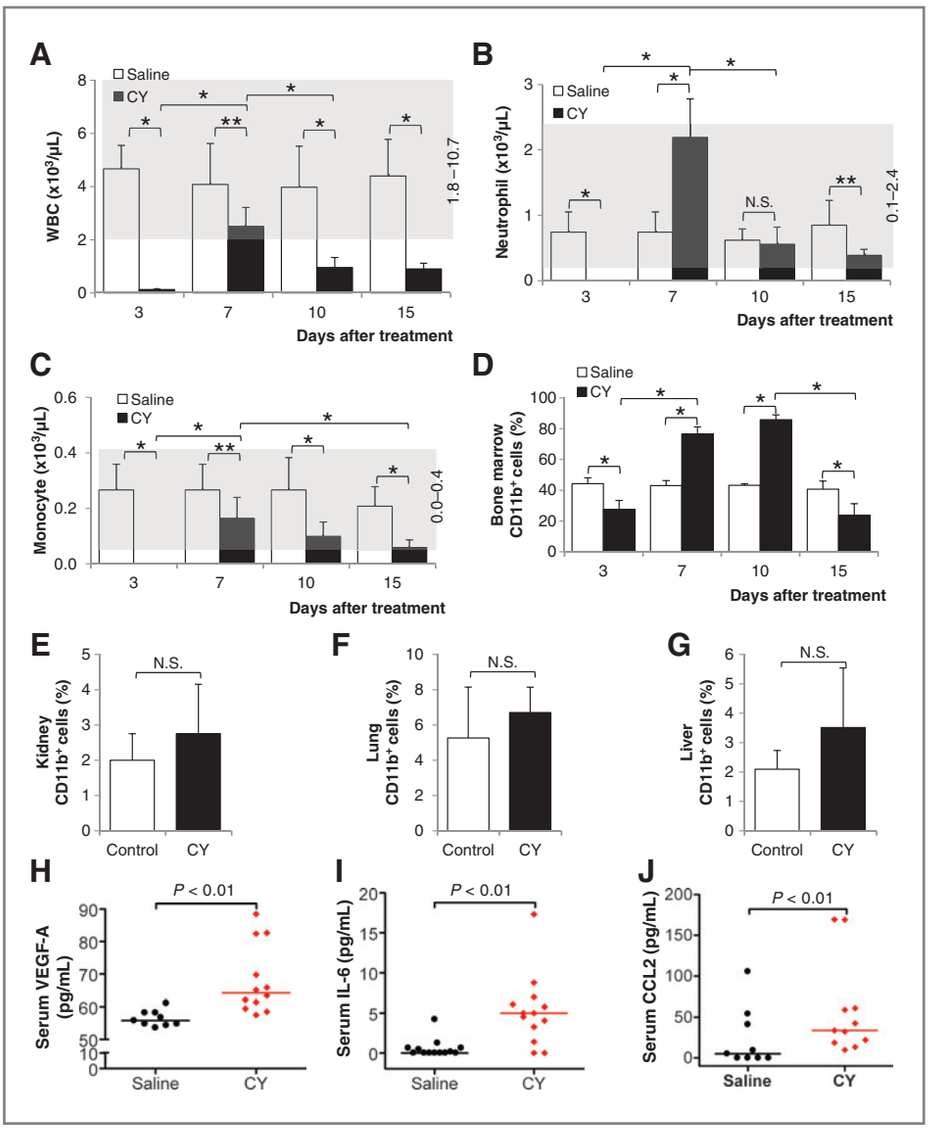

Figure 4. Cyclophosphamide (CY) transiently expanded monocytes and neutrophils in the peripheral blood and myeloid lineage cells in the bone marrow during the recovery phase after bone marrow suppression. A–C, male C57BL6/J mice ($n = 8$/group at each time point) were treated with saline (control) or CY, followed by total WBC (A), neutrophil (B), and monocyte (C) counting on 3, 7, 10, and 15 days after treatment. Data are mean ± SD. Asterisks indicate statistical significance (*, $P < 0.01$ and **, $P < 0.05$ by the Student t test). Shade indicates standard range. D, male C57BL/6J mice ($n = 8$ per group at each time point) were treated with saline (control) or CY followed by flushing bone marrow cells for flow cytometric analysis of myeloid lineage cell populations (expressing CD11b) on 3, 7, 10, and 15 days after treatment. Data are mean ± SD, and asterisks represent statistical significance (*, $P < 0.01$ and **, $P < 0.05$ by the Student t test). E–G, CY treatment did not increase $CD11b^+$ myeloid cells in solid organs. Male C57BL/6J mice ($n = 6$/group) were treated with saline (control) or CY. After 7 days, kidney (E), lung (F), and liver (G) were surgically removed and digested for flow cytometric analyses of $CD11b^+$ myeloid cells. Data are mean ± SD. N.S. indicates "not significant" by the Student t test. H–J, CY treatment increased myeloid-associated cytokines in serum. Male C57BL/6J mice ($n = 12$ each) were treated with saline (control) or CY. After 7 days, serum cytokines including VEGF-A (H), IL-6 (I), and CCL2 (J) were measured by ELISA. Each dot represents an individual serum cytokine level and bars represent median ($P < 0.01$ by Mann–Whitney U test).

cyclophosphamide administration with suppression on days 3 and 15 (Fig. 4D). In contrast, there was no change in the numbers of $CD11b^+$ cells in other organs such as kidney, lung, and liver (Fig. 4E–G). We next determined the serum protein levels of VEGF-A, IL-6, and CCL2. All 3 molecules have angiogenic properties and also promote myeloid cell proliferation and differentiation (29–31). All 3 serum cytokines were significantly increased by cyclophosphamide treatment (Fig. 4H–J).

Cyclophosphamide-induced skeletal metastases overlap temporally with bone marrow myeloid cell expansion

To assess the temporal impact of cyclophosphamide on myeloid cell populations, the effects of tumor inoculation at various times after cyclophosphamide treatment were evaluated. PC-3^{Luc} tumor cells were inoculated into the systemic circulation 3, 7, and 15 days after cyclophosphamide treatment (Fig. 5A). The 7-day group had significantly more metastases,

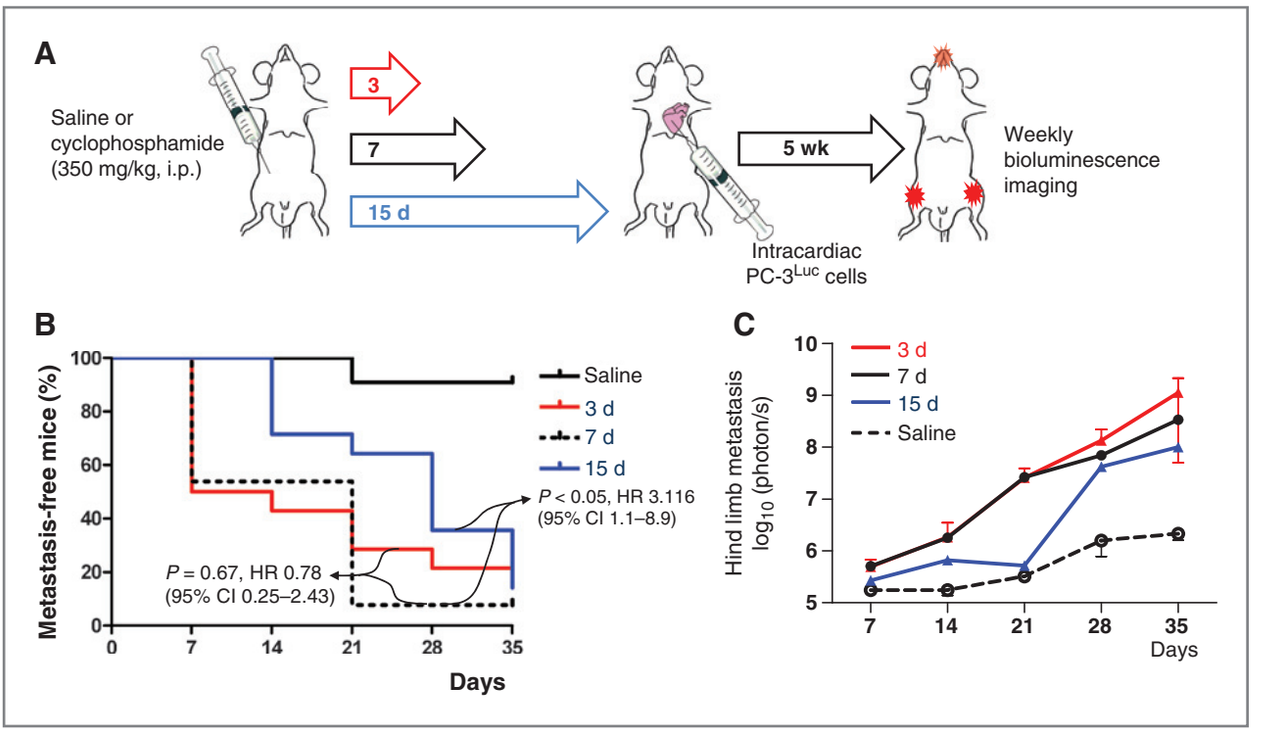

Figure 5. Recovery time after cyclophosphamide (CY) administration affected development of skeletal metastases. A, schematic representation of the experiment. Male athymic mice were treated with saline or CY. Following 3, 7, or 15 days of recovery respectively, PC-3^{Luc} tumor cells were inoculated via intracardiac injection. Development and subsequent growth of metastatic tumors were monitored by weekly *in vivo* bioluminescence imaging for 5 weeks. B, percentage of metastasis-free mice was plotted in a Kaplan–Meier survival curve. The 7-day group had significantly increased hind limb metastases compared with the saline-treated control group [$P < 0.01$ by log-rank test, HR = 0.07 with 95% confidence interval (CI), 0.02–0.25]. The 3-day group was similar to the 7-day group ($P = 0.67$ by log-rank test, HR = 0.78 with 95% CI, 0.25–2.43), whereas the 15-day group had significantly slower development of metastases than the 7-day group ($P < 0.05$ by log-rank test, HR = 3.116 with 95% CI, 1.1–8.9). C, hind limb metastatic tumor size was measured by weekly *in vivo* bioluminescence imaging. All CY-treated groups had significantly increased photon emission from the hind limbs compared with the saline-treated mice (pairwise linear contrasts $P < 0.01$ at all time points). The 3-day group had significantly increased tumor burden compared with the 7-day group on week 5 imaging (pairwise linear contrasts $P < 0.01$), whereas the 15-day group had significantly reduced tumor burden compared with the 7-day group (pairwise linear contrasts $P < 0.01$). Data are median ± interquartile range.

than the saline-treated control group, as observed previously. When tumor cells were injected at a later time point (i.e., 15 days after cyclophosphamide treatment), significantly fewer mice developed hind limb metastatic lesions, suggesting that levels of bone marrow myeloid cell populations correlate with hind limb metastases (Fig. 5B and C). The 3-day group had a similar metastatic pattern as the 7-day group (Fig. 5B) and increased tumor size compared with the 7-day group (Fig. 5C), potentially because of prolonged survival of tumor cells in the systemic circulation overriding the expansion of bone marrow myeloid cells.

Neutralizing host-derived murine CCL2, but not IL-6, inhibited cyclophosphamide-induced prostate cancer bone metastasis

These data described earlier collectively showed that cyclophosphamide provided an environment conducive to experimental prostate cancer skeletal metastasis, potentially mediated by increase of serum cytokines and/or expansion of myeloid cells. The causal relationship of alterations induced by cyclophosphamide and tumor metastasis was determined using the intracardiac metastasis model in combination with neutralizing antibodies. Mice were treated with neutralizing antibodies targeting mouse IL-6 or mouse CCL2 during the 7 day recovery phase after cyclophosphamide treatment (Fig. 6A). Consistent with the observation in Fig. 1B, cyclophosphamide treatment significantly enhanced the development and subsequent growth of experimental bone metastasis (Fig. 6B;). Neutralizing IL-6 did not prevent development of metastasis in cyclophosphamide-treated mice. However, neutralizing CCL2 significantly inhibited ~~the~~ cyclophosphamide-induced prostate cancer metastasis *in vivo* (statistical comparison shown in Fig. 6C and D), indicating that the upregulation of CCL2 in response to cyclophosphamide contributed to the development and progression of metastasis. Moreover, administration of both antibodies against IL-6 and CCL2 had similar effects to the anti-CCL2 antibody alone group (Fig. 6B–D). Importantly, neutralizing antibodies were administered before the tumor cell inoculation, to exclude the possibility of direct effects of the drug on the tumor cells. Therefore, the effects of neutralizing antibody were mainly due to the changes exerted on the host microenvironment. However, preclinical pharmacokinetic studies showed that anti-CCL2 antibody can remain detectable in serum up to 10 days after administration, thus the possibility

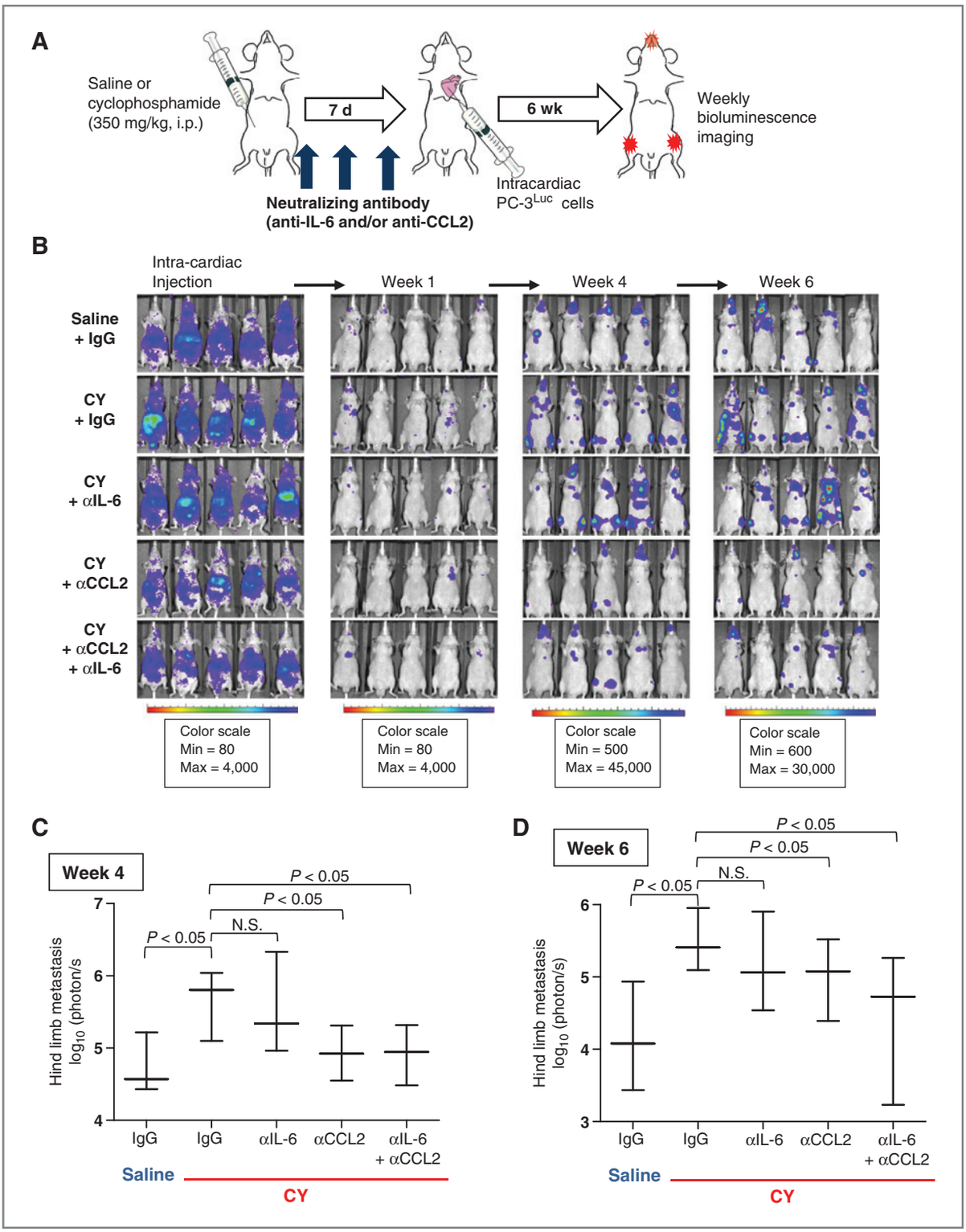

Figure 6. Neutralizing CCL2, but not IL-6, reverted cyclophosphamide (CY)-induced prostate cancer bone metastasis. A, schematic representation of the experiment. Male athymic mice were treated with saline ($n = 10$) or CY in combination with control IgG ($n = 14$; 10 mg/kg, i.p.), anti-mouse IL-6 ($n = 11$; 20 mg/kg, i.p.), anti-mouse CCL2 [$n = 12$; 10 mg/kg, intraperitoneal (i.p.)], or a combination of anti-IL-6 and CCL2 antibodies ($n = 12$). Three doses were given 1 day before CY treatment and 3 and 6 days after CY treatment. On day 7 post-CY injection, PC-3^{Luc} cells were injected into the left heart ventricle. Hind limb metastatic tumors were monitored by weekly *in vivo* bioluminescence imaging for 6 weeks. B, serial images from 5 representative mice from each group are shown. C and D, week 4 (C) and week 6 (D) bioluminescence data were quantified and plotted. Tumor size was measured by photon/s from the hind limb lesions in each group. Data are median ± interquartile range, and statistical significance was determined by Mann–Whitney *U* test.

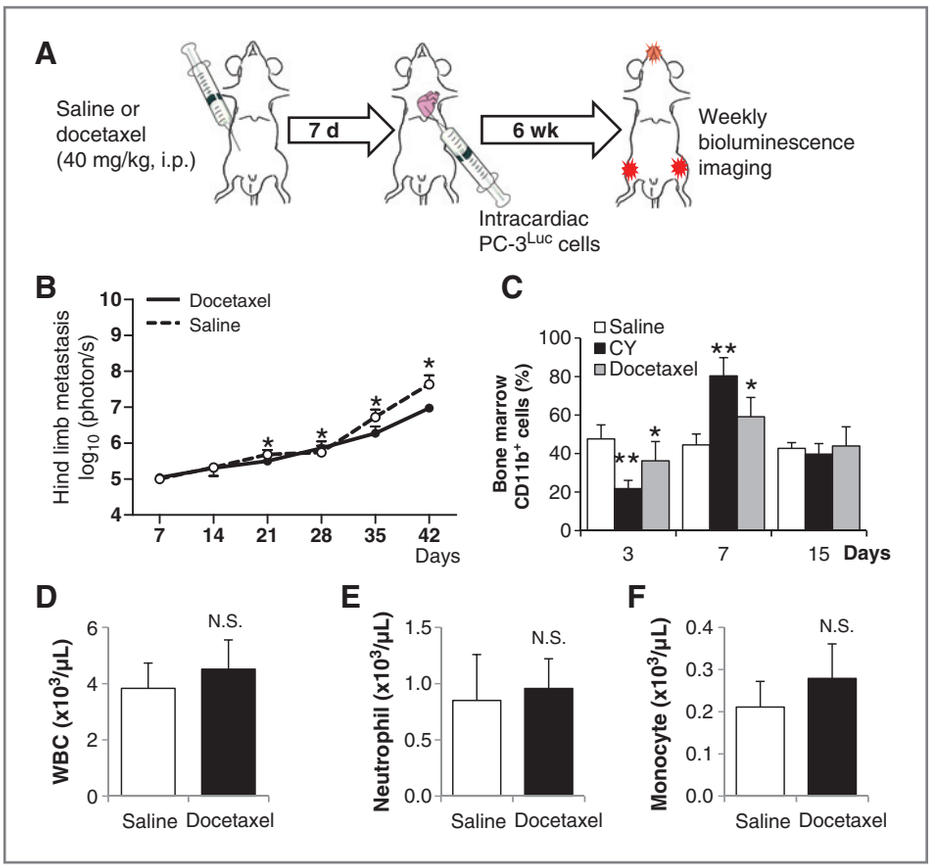

Figure 7. Docetaxel pretreatment did not promote the development of hind limb skeletal metastasis. A, schematic representation of the experiment. Male athymic mice were treated with saline or docetaxel. Following 7 days of recovery, PC-3^{Luc} cells were injected into the left heart ventricle ($n = 10$ for saline control and $n = 12$ for docetaxel group). Hind limb metastatic tumors were monitored by weekly *in vivo* bioluminescence imaging for 6 weeks. B, hind limb metastatic tumor size was measured by weekly *in vivo* bioluminescence imaging. Data are medians with interquartile range. Asterisks represent statistical significance (linear contrasts $P < 0.01$). C, docetaxel induced myeloid cell expansion similarly but to a lesser extent than cyclophosphamide (CY). Data are mean ± SD, and asterisks represent statistical significance (*, $P < 0.01$ and **, $P < 0.05$ by the Student *t* test). D–F, male C57BL6/J mice ($n = 10$/group) were treated with saline or docetaxel (40 mg/kg, i.p.) followed by complete blood counting (CBC) with WBC differential counting 7 days after treatment. The numbers of WBC (D), neutrophils (E), and monocytes (F) are plotted. Data are mean ± SD. N.S. stands for "not significant" ($P > 0.05$ by the Student *t* test).

of direct effects may not be completely excluded (personal communication).

An alternative chemotherapeutic drug, docetaxel, did not promote skeletal metastases

To further determine the causal role of cyclophosphamide-induced myeloid cell expansion to the development of skeletal metastasis, the effects of docetaxel, a chemotherapeutic agent commonly included in prostate cancer treatment regimens, were tested. In contrast to cyclophosphamide-mediated pro-metastatic effects, pretreatment of mice with docetaxel decreased hind limb skeletal metastasis (Fig. 7B). In addition, CD11b$^+$ cell enumeration in the docetaxel-treated bone marrow revealed similar but significantly blunted alterations in CD11b$^+$ cells in comparison with the effects of cyclophosphamide (Fig. 7C). Docetaxel-induced myeloid cell expansion (59.1% ± 12.1%) at day 7 was not sufficient enough to increase myeloid cells (neutrophils and monocytes) in the peripheral blood (Fig. 7D–F).

Discussion

Multiple mechanisms have been proposed to explain why bone provides a congenial metastatic microenvironment. For example, bone is enriched with cytokines and growth factors that promote tumor cell proliferation, migration, and survival (32). In addition, bone houses the primary hematopoietic organ (i.e., bone marrow), containing multiple types of progenitor cells and hematopoietic cells of various tumorigenic potential. Previously, Schneider and colleagues showed that expansion of bone marrow cellularity before inoculation of prostate tumor cells significantly promoted skeletal metastasis (20), suggesting bones with increased cellularity constitute a more congenial microenvironment for metastasis. In this context, it is reasonable to expect that cytotoxic chemotherapy and/or irradiation may impact skeletal metastasis.

This study showed for the first time that alterations induced by cyclophosphamide, a common chemotherapeutic drug, enhanced prostate cancer skeletal metastasis. Furthermore, we showed that the prometastatic effects of cyclophosphamide

were significantly reversed by suppression of CCL2, which suggests the causal role of bone marrow myeloid lineage cell expansion. We showed that a single dose of cyclophosphamide administration increased myelogenic cytokines, and correspondingly expanded the myeloid cell population in the bone marrow, as well as the numbers of monocytes and neutrophils transiently in the peripheral blood.

The unexpected "opposite" protumorigenic effect of such a chemotherapeutic drug is not a novel observation in other nonskeletal sites. There have been several reports of chemotherapy-induced metastasis and/or tumor growth (18, 19, 33, 34). Most notably, Carmel and Brown showed that pretreatment of the host with cyclophosphamide, among many other chemotherapeutic drugs including actinomycin D, vinblastine, bleomycin, methotrexate, and 5-fluorouracil, resulted in the most prominent prometastatic effects in a syngeneic sarcoma lung metastasis model (17). While most of the previous studies focused on an experimental pulmonary metastasis model, our data expanded the earlier observations by showing the prometastatic effects of chemotherapy in a skeletal metastasis model (Fig. 1 and Supplementary Fig. S3). Data in the present study suggest that chemotherapeutic drugs with strong bone marrow suppression may have the adverse effect of promoting bone metastasis, a finding which has not been extensively investigated. Cyclophosphamide is not a standard chemotherapeutic drug for patients with prostate cancer, but recently low-dose metronomic administration of cyclophosphamide is in clinical trials as an antiangiogenic therapy in prostate cancer (35, 36). In addition, cyclophosphamide is widely used for treatment of breast cancer, which also has a strong propensity for skeletal metastasis. Consequently, the effects of varying dosages and administration scheduling of cyclophosphamide on bone metastasis warrant extensive further studies.

The findings concerning the mechanisms involved in chemotherapy-enhanced metastasis have clinically therapeutic implications. We showed that the numbers of bone marrow myeloid cells and myelomonocytic cells in the peripheral blood are significantly increased after cyclophosphamide administration, but not after docetaxel administration, potentially mediated by the increase of myelogenic cytokines. During the recovery phase after bone marrow suppression, spikes of monocytes and neutrophils are frequently observed in patients, and clinically considered a favorable prognostic sign (37). Data in the present study confirmed an abrupt increase of neutrophils and monocytes shortly after cyclophosphamide administration. Moreover, significant increases in CCL2, IL-6, and VEGF-A, all of which are potent myelogenic factors, were observed simultaneously or before the expansion of myelomonocytic cells, supporting the roles of these factors in the expansion of $CD11b^{+}$ myeloid cells in the bone marrow. Results of this work confirmed that neutralizing CCL2, but not IL-6, significantly inhibited the prometastatic effects of cyclophosphamide. It should be noted that anti-CCL2 antibody is specific to the murine host–derived CCL2, and does not cross-react with prostate cancer-derived human CCL2, and that the neutralizing antibody was administered in only 3 dosages before tumor cell inoculation. Collectively, these data suggest that neutralizing CCL2 reconditions the premetastatic host microenvironment induced by chemotherapy.

Although the present data show the efficacy of anti-CCL2 antibody in the cyclophosphamide-induced prostate cancer bone metastasis model, increased expression of CCL2 (and subsequent expansion of myeloid cells) may not be the only mechanism of promoting metastasis after cyclophosphamide treatment. The first alternative explanation for the prometastatic effects of cyclophosphamide is that it could be mediated by the effects on bone cells. Given that inhibition of osteoclasts reversed the effects of granulocyte macrophage colony-—stimulating factor (GM-CSF) on metastasis in a mouse model (38), it is possible that the effects of CCL2 neutralizing antibody in these results were, in part, mediated by inhibition of osteoclastogenesis. Second, while our results failed to confirm the causal role of cyclophosphamide-induced endothelial damage in metastasis, the possibility still remains for further investigation. Cyclophosphamide is currently being tested for efficacy as antiangiogenic therapy, and disruption of endothelial barrier function can promote extravasation of tumor cells in the metastatic microenvironment. Previously, Shirota and Tavassoli showed that cyclophosphamide induces endothelial damage detectable by electron microscopy, and destroys the integrity of bone marrow sinus endothelium (indicated by red blood cells in the extravascular space), leading to enhanced engraftment of bone marrow transplantation (28). Therefore, cyclophosphamide effects on metastasis may be varied in different dosing schedules (i.e., metronomic low dose) or different tumor models.

In conclusion, this study showed that priming the murine host with cyclophosphamide altered the bone microenvironment, leading to promotion of prostate cancer bone metastasis. In addition, suppression of host CCL2 by antibody treatment significantly reduced the adverse effects of cyclophosphamide.

Disclosure of Potential Conflicts of Interest

Q5

L.A. Snyder and J.A. Nemeth are employed by Janssen, LLC. K.J. Pienta is the consultant/advisory board member for Curis. L.K. McCauley ~~has~~ commercial research grant ~~for~~ Centocor. No potential conflicts of interest were disclosed by the other authors.

Authors' Contributions

Q6

Conception and design: S.I. Park, J. Liao, J.A. Nemeth, L.A. Snyder, K.J. Pienta, L.K. McCauley
Development of methodology: S.I. Park, J. Liao, J.E. Berry, L.K. McCauley
Acquisition of data (provided animals, acquired and managed patients, provided facilities, etc.): S.I. Park, J. Liao, J.E. Berry, X. Li, A.J. Koh, M.E. Michalski, M.R. Eber, F.N. Soki, S. Sud, T.J. Wronski
Analysis and interpretation of data (e.g., statistical analysis, biostatistics, computational analysis): S.I. Park, J. Liao, S. Daignault-Newton, T.J. Wronski, K.J. Pienta, L.K. McCauley
Writing, review, and/or revision of the manuscript: S.I. Park, J. Liao, J.E. Berry, M.E. Michalski, D. Sadler, J.A. Nemeth, L.A. Snyder, T.J. Wronski, L.K. McCauley
Administrative, technical, or material support (i.e., reporting or organizing data, constructing databases): S.I. Park, A.J. Koh, D. Sadler, S. Tisdelle, L.K. McCauley
Study supervision: S.I. Park, L.K. McCauley

Acknowledgments

The authors thank Rashesh Kapadia for μCT scanning, Evan Keller and Russell Taichman for discussions, and Chris Strayhorn for histology.

Grant Support

This work was financially supported by the Department of Defense W81XWH-10-1-0546 (to S.I. Park) and W81XWH-08-1-0037 (to L.K. McCauley); the National Cancer Institute P01CA093900 (to K.J. Pienta and L.K. McCauley) and P50CA69568 (to K.J. Pienta); American Cancer Society Clinical Research Professorship (to K.J. Pienta); and Janssen (L.K. McCauley).

The costs of publication of this article were defrayed in part by the payment of page charges. This article must therefore be hereby marked *advertisement* in accordance with 18 U.S.C. Section 1734 solely to indicate this fact.

Received September 1, 2011; revised January 9, 2012; accepted January 31, 2012; published OnlineFirst xx xx, xxxx.

References

1. Hess KR, Varadhachary GR, Taylor SH, Wei W, Raber MN, Lenzi R, et al. Metastatic patterns in adenocarcinoma. Cancer 2006;106:1624–33.
2. Weilbaecher KN, Guise TA, McCauley LK. Cancer to bone: a fatal attraction. Nat Rev Cancer 2011;11:411–25.
3. Roodman GD. Mechanisms of bone metastasis. N Engl J Med 2004;350:1655–64.
4. Park SI, Soki FN, McCauley LK. Roles of bone marrow cells in skeletal metastases: no longer bystanders. Cancer Microenviron 2011;4:237–46.
5. Seandel M, Butler J, Lyden D, Rafii S. A catalytic role for proangiogenic marrow-derived cells in tumor neovascularization. Cancer Cell 2008;13:181–3.
6. Yang L, DeBusk LM, Fukuda K, Fingleton B, Green-Jarvis B, Shyr Y, et al. Expansion of myeloid immune suppressor Gr+CD11b+ cells in tumor-bearing host directly promotes tumor angiogenesis. Cancer Cell 2004;6:409–21.
7. Ahn GO, Brown JM. Matrix metalloproteinase-9 is required for tumor vasculogenesis but not for angiogenesis: role of bone marrow-derived myelomonocytic cells. Cancer Cell 2008;13:193–205.
8. Ahn GO, Tseng D, Liao CH, Dorie MJ, Czechowicz A, Brown JM. Inhibition of Mac-1 (CD11b/CD18) enhances tumor response to radiation by reducing myeloid cell recruitment. Proc Natl Acad Sci U S A;107:8363–8.
9. Kozin SV, Kamoun WS, Huang Y, Dawson MR, Jain RK, Duda DG. Recruitment of myeloid but not endothelial precursor cells facilitates tumor regrowth after local irradiation. Cancer Res 2010;70:5679–85.
10. Ahn GO, Brown JM. Influence of bone marrow-derived hematopoietic cells on the tumor response to radiotherapy: experimental models and clinical perspectives. Cell Cycle 2009;8:970–6.
11. Mizutani K, Sud S, McGregor NA, Martinovski G, Rice BT, Craig MJ, et al. The chemokine CCL2 increases prostate tumor growth and bone metastasis through macrophage and osteoclast recruitment. Neoplasia 2009;11:1235–42.
12. Mizutani K, Sud S, Pienta KJ. Prostate cancer promotes CD11b positive cells to differentiate into osteoclasts. J Cell Biochem 2009;106:563–9.
13. Zhang J, Lu Y, Pienta KJ. Multiple roles of chemokine (C-C motif) ligand 2 in promoting prostate cancer growth. J Natl Cancer Inst 2010;102:522–8.
14. Richman CM, Weiner RS, Yankee RA. Increase in circulating stem cells following chemotherapy in man. Blood 1976;47:1031–9.
15. Abrams RA, Johnston-Early A, Kramer C, Minna JD, Cohen MH, Deisseroth AB. Amplification of circulating granulocyte-monocyte stem cell numbers following chemotherapy in patients with extensive small cell carcinoma of the lung. Cancer Res 1981;41:35–41.
16. Vollmer TL, Conley FK. Effect of cyclophosphamide on survival of mice and incidence of metastatic tumor following intravenous and intracardial inoculation of tumor cells. Cancer Res 1984;44:3902–6.
17. Carmel RJ, Brown JM. The effect of cyclophosphamide and other drugs on the incidence of pulmonary metastases in mice. Cancer Res 1977;37:145–51.
18. Wu YJ, Muldoon LL, Dickey DT, Lewin SJ, Varallyay CG, Neuwelt EA. Cyclophosphamide enhances human tumor growth in nude rat xenografted tumor models. Neoplasia 2009;11:187–95.
19. Yamauchi K, Yang M, Hayashi K, Jiang P, Yamamoto N, Tsuchiya H, et al. Induction of cancer metastasis by cyclophosphamide pretreatment of host mice: an opposite effect of chemotherapy. Cancer Res 2008;68:516–20.
20. Schneider A, Kalikin LM, Mattos AC, Keller ET, Allen MJ, Pienta KJ, et al. Bone turnover mediates preferential localization of prostate cancer in the skeleton. Endocrinology 2005;146:1727–36.
21. Park SI, Kim SJ, McCauley LK, Gallick GE. Pre-clinical mouse models of human prostate cancer and their utility in drug discovery. Curr Protoc Pharmacol 2011;51:145–527.
22. Guldberg RE, Duvall CL, Peister A, Oest ME, Lin AS, Palmer AW, et al. 3D imaging of tissue integration with porous biomaterials. Biomaterials 2008;29:3757–61.
23. Loberg RD, Ying C, Craig M, Day LL, Sargent E, Neeley C, et al. Targeting CCL2 with systemic delivery of neutralizing antibodies induces prostate cancer tumor regression *in vivo*. Cancer Res 2007;67:9417–24.
24. Li X, Loberg R, Liao J, Ying C, Snyder LA, Pienta KJ, et al. A destructive cascade mediated by CCL2 facilitates prostate cancer growth in bone. Cancer Res 2009;69:1685–92.
25. Tsui P, Das A, Whitaker B, Tornetta M, Stowell N, Kesavan P, et al. Generation, characterization and biological activity of CCL2 (MCP-1/JE) and CCL12 (MCP-5) specific antibodies. Hum Antibodies 2007;16:117–25.
26. Bagley CM Jr, Bostick FW, DeVita VT Jr. Clinical pharmacology of cyclophosphamide. Cancer Res 1973;33:226–33.
27. Kline I, Gang M, Tyrer DD, Mantel N, Venditti JM, Goldin A. Duration of drug levels in mice as indicated by residual antileukemic efficacy. Chemotherapy 1968;13:28–41.
28. Shirota T, Tavassoli M. Cyclophosphamide-induced alterations of bone marrow endothelium: implications in homing of marrow cells after transplantation. Exp Hematol 1991;19:369–73.
29. Ferrara N, Gerber HP, LeCouter J. The biology of VEGF and its receptors. Nat Med 2003;9:669–76.
30. Kim S, Takahashi H, Lin WW, Descargues P, Grivennikov S, Kim Y, et al. Carcinoma-produced factors activate myeloid cells through TLR2 to stimulate metastasis. Nature 2009;457:102–6.
31. Roca H, Varsos ZS, Sud S, Craig MJ, Ying C, Pienta KJ. CCL2 and interleukin-6 promote survival of human CD11b+ peripheral blood mononuclear cells and induce M2-type macrophage polarization. J Biol Chem 2009;284:34342–54.
32. Chantrain CF, Feron O, Marbaix E, Declerck YA. Bone marrow microenvironment and tumor progression. Cancer Microenviron 2008;1:23–35.
33. Man S, Zhang Y, Gao W, Yan L, Ma C. Cyclophosphamide promotes pulmonary metastasis on mouse lung adenocarcinoma. Clin Exp Metastasis 2008;25:855–64.
34. van Putten LM, Kram LK, van Dierendonck HH, Smink T, Fuzy M. Enhancement by drugs of metastatic lung nodule formation after intravenous tumour cell injection. Int J Cancer 1975;15:588–95.
35. Emmenegger U, Morton GC, Francia G, Shaked Y, Franco M, Weinerman A, et al. Low-dose metronomic daily cyclophosphamide and weekly tirapazamine: a well-tolerated combination regimen with enhanced efficacy that exploits tumor hypoxia. Cancer Res 2006;66:1664–74.
36. Lord R, Nair S, Schache A, Spicer J, Somaihah N, Khoo V, et al. Low dose metronomic oral cyclophosphamide for hormone resistant prostate cancer: a phase II study. J Urol 2007;177:2136–40.
37. McClatchey KD, editor. Clinical laboratory medicine. Philadelphia, PA: Lippincott Williams & Wilkins; 2001.
38. Dai J, Lu Y, Yu C, Keller JM, Mizokami A, Zhang J, et al. Reversal of chemotherapy-induced leukopenia using granulocyte macrophage colony-stimulating factor promotes bone metastasis that can be blocked with osteoclast inhibitors. Cancer Res 2010;70:5014–23.